ISSN 1849–0751 (On–line)
ISSN 0013–7448 (Print)
UDK 621.31

https://doi.org/10.37798/EN2024731

Journal of Energy

VOLUME 73 Number 1 | 2024

ENERGIJA 73

Journal of Energy

Scientific Professional Journal Of Energy, Electricity, Power Systems
Online ISSN 1849–0751, Print ISSN 0013–7448, VOL 73
https://doi.org/10.37798/EN2024731

Published by
HEP d.d., Ulica grada Vukovara 37, HR–10000 Zagreb
HRO CIGRÉ, Berislavićeva 6, HR–10000 Zagreb

EDITORIAL

The first paper is “New Transformer Procurement Concepts in Times of High Uncertainty and Market Instability”. The concept of standard transformer design defined in this paper has proven to be a successful strategy at SP Energy Networks to place orders for power transformers early enough to ensure that the business capital investment plans can be implemented according to the agreed programs and that price uncertainties and the associated commercial risks are appropriately shared between manufacturer and purchaser. This approach and its repeatability, together with a stable supplier base, help to shorten tendering timescales in multiple tender event situations and reduce resource deployment requirements, not only at the tendering stage but potentially also in the subsequent evaluation of equipment and substation development after contract award.

The second paper is “Hybrid Analytical-FEM Approach for Power Transformer Transient Analysis”. The paper presents a novel high-frequency model to accurately predict the transient behavior of transformer windings down to the turn level. It uses lumped RLC parameters that are analytically derived and solved in the time domain. To increase the accuracy, correction factors derived from numerical simulations are included. Validation is carried out by measurements on a disk winding of a power transformer. The capacitances are estimated analytically using correction factors from 2D FEM, while the inductances and resistances are calculated analytically, neglecting the permeable core for high-frequency transients. This approach enables fast calculations, even for complex winding geometries, so that it can be used in the design of transformers, with parameter calculations taking only seconds and time domain calculations taking only tens of seconds.

The third article is entitled “Measurement Uncertainty in On-line Bushing Monitoring”. Recent monitoring units show that the uncertainty of station voltage measuring transformers significantly affects the overall uncertainty budget, regardless of the measurement method used. Correcting network unbalance, either by separate voltage phase measurements or by phasor techniques, significantly improves the assessment of the dielectric dissipation factor (tgδ) and capacitance factor (C) of bushings. Effective correction of power network unbalance is crucial for reliable results when assessing bushing condition in online monitoring systems. Calibration is essential to offset constant errors introduced by individual system components. In addition, the uncertainties of the voltage transformer parameters and temperature effects must be taken into account when defining the uncertainty budget. These measures ensure the accuracy and reliability of high voltage bushing insulation indicators in online monitoring systems.

The fourth paper is “Improving the Reliability of Online Bushing Monitoring”. This paper addresses the widespread problem of bushing failures in power transformers and proposes methods to mitigate such failures through online monitoring. A technique is presented that compares the bushing leakage currents of different transformers connected to the same busbars. This is intended to solve problems arising from unreliable measurement results due to grid voltage imbalances or frequent transformer outages. This method has several improvements over the conventional three-phase bank approach. It offers higher reliability and significantly faster response times and enables the measurement of the temperature dependence of the power factor - a potential early indicator of moisture ingress into bushings. Compared to alternative reference methods, it boasts lower complexity and lower implementation costs, while allowing for straightforward upgrades to existing monitoring systems.

The last article is entitled “Is Nuclear Fusion Losing the Race with Global Warming?”. Nuclear fission, a proven technology, is a viable solution to mitigate the effects of climate change until fusion energy becomes commercially viable. While the authors are optimistic about the potential of nuclear fusion, they argue for a realistic assessment of the timeframe. In the meantime, it is important to use emission-free sources such as safe nuclear fission under the supervision of the IAEA. Solar energy, including ocean heat, should be developed more independently of the day-night cycle. The proposal to build one hundred nuclear fission power plants by 2034-2063/65 shows the potential for rapid progress in combating global warming. Advanced nuclear fission power plants could provide a valuable head start in the race against climate change if nuclear fusion is delayed. Given the urgency, decision-makers need to allow for a preparation time of at least several years, preferably no shorter than five years before 2055, in case fusion proves unachievable within a reasonable timeframe.

Igor Kuzle
Editor–in–Chief

Journal of Energy

VOLUME 73 Number 1 | 2024

journal homepage: http://journalofenergy.com/

New Transformer Procurement Concepts in Times of High Uncertainty and Market Instability

Jose Quintana, Wilson Smith, Mateja Cepin

***Summary* — New and proactive strategies are required in utilities and other transformer purchasers to ensure delivery of transformer capital investment plans in the current times of market saturation and various supply chain issues. Close collaboration with suppliers and adaptative and flexible engineering and commercial initiatives need to be implemented from as early stage in the project lifecycle as definition of requirements and tendering. This paper presents the strategy adopted by SP Energy Networks, and one of their main suppliers of power transformers, Kolektor Etra, in this regard.**

***Keywords* — Transformer, Procurement, Standardisation, CPA, supply chain**

I. Introduction

Traditional procurement strategies in the area of power transformers have been proven to be no longer adequate to facilitate delivery of capital investment plans in the current climate of market saturation and various supply chain issues. Increasing demand worldwide in order to facilitate the green energy transition plans defined by the different national governments or institutions compounded by the multiple and unique market disruptive events that have been experienced in the recent years (i.e. COVID-19, Ukraine/Russia conflict, expansion of other related manufacturing industries…) have placed the power transformer industry supply chain under significant strain. Unit costs and lead times for power transformers have been seen to more than double in the shorter space of less than a year. These significant changes in the market environment need to be acknowledged by purchasers and manufacturers equally and adaptative and flexible approaches put in place in order to mitigate commercial and project delivery risks whilst maintaining quality standards and resilience of the equipment to be installed in the electricity networks. All the different areas associated with the procurement of new power transformers (i.e. technical specifications, supplier qualification, commercial requirements, project planning…) need to be included within this review and modification of current practices.

This paper provides an overview of the strategy adopted by SP Energy Networks, distribution and transmission network operator in the United Kingdom, and one of their main power transformer suppliers in the current period, Kolektor Etra from Slovenia.

(Corresponding author: Jose Quintana)

Jose Quintana and Wilson Smith are with the SP Energy Networks, Scottish Power HQ, Glasgow, United Kingdom (e-mails: jquintana@spenergynetworks.co.uk, Wilson.Smith@scottishpower.com)

Mateja Čepin is with the Kolektor Etra, Ljubljana, Slovenia (e-mail: Mateja.Cepin@kolektor.com)

II. Adaptative Strategies on Technical Areas

Review of transformer fleet and associated technical parameters

One of the main aspects influencing the efficiency of the power transformers procurement process is the degree of standardization achieved in the purchaser's network. Situations where transformers are purchased on a one-off basis with individual technical specifications and ad-hoc requirements to suit specific network conditions, substation locations and/or installation environments require significant engineering efforts. This additionally multiplies the number of tender events required and variety of transformers included within, which translates into a higher workload for both purchaser and manufacturer during each individual tender event and slow down the overall process.

In order to minimise this type of situations, it is important that the purchaser carry out an upfront holistic review of its network requirements with the aim of optimizing the number of asset types required while still ensuring network performance and license obligations are fulfilled. This not only assists in tendering processes but on the overall fleet management (i.e. monitoring and cross-reference of sister units, business strategy on strategic spares…). Certain transformer design parameters are dictated by the historical network construction (i.e. voltage class, insulation levels, etc.) with not much possibility to deviate from. However, others offer a greater degree of flexibility and can be defined with an overall view of present and future needs in order to identify the most optimum set of requirements, not for each individual substation, but for the network as a whole. Example of these could be impedance, rated power, tapping range, sound power level, etc. Although it is possible to define these on a site-specific basis, it is also possible to undertake a commonality analysis with the aim of identifying a suitable set of requirements to encompass a larger number of possible applications, or at least, establish a limited number of set of requirements. Caution shall be applied not to select worst case scenario type characteristics as otherwise a large number of new transformers can end up being significantly overspecified with the associated commercial implications. Figure 1 shows a real example where the different impedance envelopes required for two different transformers were overlapped and a common compliance area identified across the more relevant tap positions. The two transformers could be specified with a single more restrictive impedance envelope, obtaining a one design fit both type of solution. This design could also be adopted in subsequent projects requiring this type of transformer. This has the associated commercial benefits of only one design cost, only one type test costs, only one civil and P&C design cost... Although this exercise seems simple, the technical feasibility of a more restrictive impedance envelope should

Jose Quintana, Wilson Smith, Mateja Cepin, New Transformer Procurement Concepts in Times of High Uncertainty and Market Instability, Journal of Energy, vol. 73 Number 1 (2024), 3–7
https://doi.org/10.37798/2024731504

be discussed with the potential manufacturers, specially if allowable tolerances are narrower than those allowed by the applicable international standard. Similar case could be discussed in terms of specifying rated power. A selection of rated power requirements with adequate step increases (i.e. 60MVA, 90MVA, 120MVA, etc.) would be more efficient for a network operator than individually specifying based on current or forecasted site load (i.e. 52MVA, 57MVA, 62MVA instead of 60MVA for all). Any cost premium derived from specifying a slightly higher rated power than required will be most likely offset by the efficiencies gain in design standardization unless the step change is very significant. A cost-benefit analysis can be conducted to confirm that is the case.

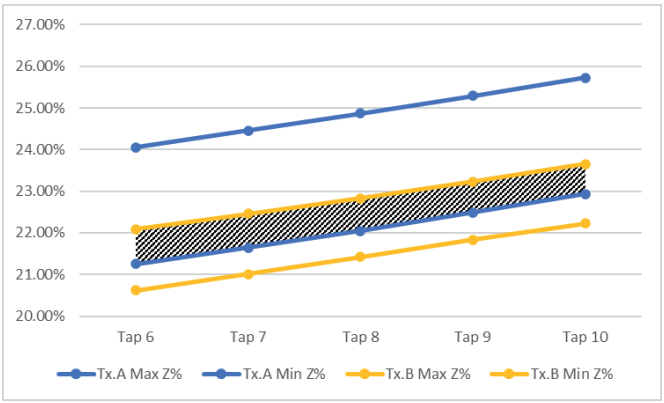

Fig. 1. Example of overlapping impedance envelopes and common compliance area for the original 275/33kV 120MVA transformer replacement requirements at East Kilbride and Dewar Place substations

The purchaser may be tempted to follow a like-for-like approach on transformer replacement projects on the assumption that the existing transformer type is the best possible solution for the site in question. However, this may not necessarily be correct as network operating conditions and requirements may have changed during the lifetime of the asset now being replaced, meaning that a different selection may be more adequate. This is especially relevant where the purchaser faces the replacement of legacy transformer types, with only a small number installed in the network and that are no longer purchased for new substations. In these cases, it is even more advisable to carry out the previously mentioned holistic review to try to progressively remove these legacy types of transformers from the network. However, in certain situations this may require a complete re-design of the network in the specific area where these legacy types can be found, including network voltage upgrades/downgrades, circuit reconfiguration, substation removal and relocation, etc. As an example, in SP Energy Networks the 132/33kV 45MVA legacy transformer type (6 units in total) is planned to be replaced, once end of life conditions reached, with a standard 132/33kV 60MVA transformer type as purchase cost differential in this case is considered to be offset by the standardisation related savings.

In the particular case of SP Energy Networks, as outcome of this holistic network review exercise and standardisation strategy, a standard list of transmission class transformer types was produced, and all key associated electrical parameters specified (i.e. voltage class, insulation levels, rated power, impedance envelope, tapping range, etc.). This list comprises 5 off types of 400kV and 275kV autotransformers and 11 off types of 275kV and 132kV double-wound transformers. It shall be mentioned this list is not rigid, and there may be situations where special requirements for a particular site may arise, and the associated transformers have to be facilitated. However, the simple fact of deviating from the standard transformer types imposes the need for adequate technical justification to be presented and agreed with all relevant stakeholders within the business.

It is appreciated that the standardization strategy explained above may be more applicable to network operators than other potential type of purchasers (i.e. industrial customers, renewable sector, etc.) due to the larger volume of assets in ownership. However, the same principles and logic can be still applied with the required adjustment to the scale of the fleet and the specific business operating environment.

A. Standard Transformer Concept

This standardisation exercise, defining the main types of transformers required, is the first stage to minimize the number of tender events required to meet business needs. However, within each individual transformer type, there may be multiple variants associated to accommodate the transformers into the different substations they have been ordered for. On green field type substation projects or substation extension projects, the flexibility at substation design phase is such that alignment with modern design practices and use of the most optimum, both technically and commercially, transformer design is possible. However, on existing substations with in-situ transformer replacements projects, or where extension of the substation platform is not possible, the available layout is already given, and additional site-specific requirements need to be considered into the project specification. This may translate into a single transformer type having different constructional variants to suit project specific requirements. There may be situations where these additional requirements drive a fundamental change of the transformer electrical design (i.e. very restrictive footprint dimensions which require re-design of the active part, use of alternative insulating fluids due to fire risk or environmental reasons, very restrictive sound power levels due to site sensitivity, etc.). However, in the majority of cases, the changes required are either mainly related to the external layout and disposition of elements (i.e. separate cooler bank vs. tank-attached radiators, cable or open air/oil bushings connection, requirement of additional online monitoring devices, etc.) or associated with the protection schemes (i.e. CT specifications).

In this second group of site-specific requirements, the electrical design of the transformer remain the same and as such the overall design of the transformer remains fundamentally the same. In the past, the Procurement strategy followed in SP Energy Networks required the transformers to be individually specified for each individual substation project for tendering, so that all details and requirements were defined before issuing the tender enquiry to the market. This represents an issue in the current climate where the strain on the power transformer supply chain requires all orders to be placed well in advance of the actual delivery dates. As an illustrative figure, lead times for 132kV voltage class power transformers have on average increased from 8 months to 20+ months. Unfortunately, in many cases it is not possible to finalise the full substation design process, which will identify all site-specific requirements for the transformer, that far in advance.

In order to overcome this situation, and with the aim to de-couple, to an extent, the substation design process from the transformer ordering process, the standard transformer design concept was adopted in SP Energy Networks. For each transformer type, a set of requirements, which would normally be site specific, are defined assuming modern substation design practices can be applied and considering the lowest cost option for each of the requirements. For each transformer type, these requirements are as follows: tank-attached radiators; oil/air HV and LV bushings, no support brackets for tank-mounted surge arresters, standard CT specification, single gas online DGA monitoring device, and no winding hot-spot fibre optics monitoring device. A transformer type with these characteristics will be considered a standard transformer design for a generic SP Energy Networks substation and is what asked to price

Jose Quintana, Wilson Smith, Mateja Cepin, New Transformer Procurement Concepts in Times of High Uncertainty and Market Instability, Journal of Energy, vol. 73 Number 1 (2024), 3–7
https://doi.org/10.37798/2024731504

against in a tender event. This would represent the minimum cost option for a transformer compliant with SP Energy Networks specifications and requirements.

This alone represents a significant reduction in tender timescales as no longer is necessary to finalise the full substation design before going out to the market. Depending on internal governance processes of each purchaser, this can translate into almost a full year reduction in tendering timescales, which in turn allows suppliers to secure manufacturing slots far earlier to compensate for extended lead times.

B. Flexibility Mechanisms

However, as previously explained, the standard design concept may not be suitable for all sites in real life. This can be managed by the use of optional elements. All requirements that would normally be site specific, but that have been defined as part of the standard design concept, will be listed separately and tenderers advised that other possible options may be selected at the time of order. For example, three off the same transformer type are required to be ordered for three different substations, all defined as a standard design at the time of tender, but after finalization of the full substation design, it is determined two of them require a separate cooler bank rather than tank-attached radiators, and the pipework orientation and distance between main tank and cooler bank are different for each one. This information is not critical to be known at the time of tender as the fundamental transformer design remains the same, and can be provided at a later stage, after contract award and prior to commencement of the detailed design activities at the manufacturer side. As a separate cooler bank represents an additional cost compared to the requirement of the standard design concept, this would need to be managed and controlled. Firstly, by requesting prices for the optional items at time of tender, so that these are presented in advance, and secondly, by engaging and making the situation clear to the relevant project managers of the involved projects so that contract variations can be agreed to manage the commercial side. Figure 2 shows as an example the design proposal from Kolektor Etra for the case above, where the same 275kV voltage class transformer design, including main tank mechanical design, could be employed with either tank-attached radiators or separate cooler bank arrangements.

This type of strategy also assists in achieving design efficiencies, not only at the manufacturer side, but also at the purchaser side (i.e. standardization of civil and P&C arrangements, optimization of equipment assessment activities in terms of design reviews and type testing, etc.) and also facilitate a higher degree of interchangeability. For example, there may be situations where multiple transformers of the same type are on order with the same manufacturer. If the only differences across these relate to the optional items listed above, these would be easily interchangeable between projects which allows a more efficient use of the manufacturing capacity by swapping manufacturing slots where project delays are communicated, which in turn also reduces potential storage costs for the purchaser.

Another element of the standard design concept is the use of a generic substation location for pricing purposes. At the time of tender, especially on green field type substation projects, the substation location may not have been defined yet, and even if it has, the access route to it may not have been built. This makes pricing for transport and delivery especially complicated and time consuming for the manufacturer that will quite likely need to make assumptions and increase their risks provisions for any potential eventuality that may be faced. This eventually translates into an increased price for the purchaser, that may or may not materialize in real terms, but whose costs will be incurred regardless. In order to mitigate these transport related risks for both parties, a generic substation location can be defined which will be representative of a typical location and will be the basis of the commercial offer. In order for this approach to be satisfactory, a good and close working relationship between manufacturer and purchaser is required so that final actual costs are as transparent as possible and are truly reflective of the costs incurred by the transformer manufacturer. This approach has the disadvantage of leaving an open-ended cost that in certain situations can be quite significant, particularly for remote locations or locations where there is not an already existing suitable route. It may not be possible to anticipate these costs in advance without detailed route surveys, which may represent a risk for project budget and programme and should be considered on an individual basis.

C. De-Coupling Technical and Commercial Tender Phases

The standard design concept approach can also have long-term advantages in case of multiple tender events. As both transformer types and standard requirements are defined and fixed, the technical offers and design proposals submitted by the manufacturers can be re-utilised at multiple tender events. Assuming there are no fundamental changes in the purchaser technical specifications, and/or in the applicable international standards and regulations, and that there has not been any critical update in the manufacturer design policies or manufacturing techniques, the tender technical proposals would continue remaining valid from one tender event

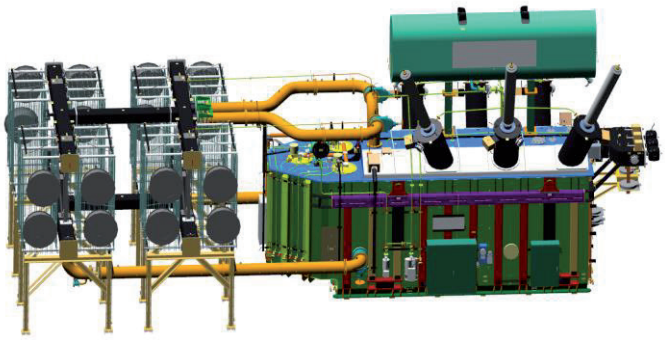

275/132/33kV 240MVA Transformer design with separate cooler bank

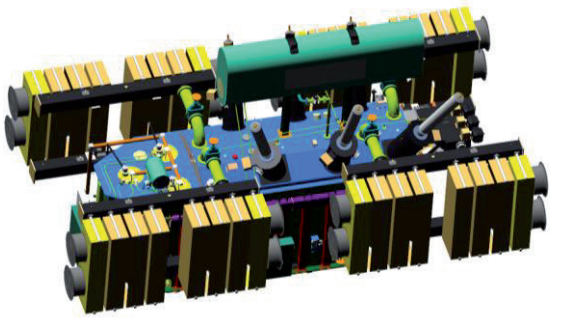

275/132/33kV 360MVA Transformer design with tank-attached radiators

Fig. 2. Illustration of the flexibility achieved by the standard design concept to accommodate different cooling arrangements

Jose Quintana, Wilson Smith, Mateja Cepin, New Transformer Procurement Concepts in Times of High Uncertainty and Market Instability, Journal of Energy, vol. 73 Number 1 (2024), 3–7
https://doi.org/10.37798/2024731504

to the following. This has resource saving advantages for both parties, i.e. the manufacturer do not need to prepare a design proposal in each tender event, and the purchase do not need to assess compliance of the same in each tender event. This allows the purchaser to build a catalogue of technically compliant proposals on the very first tender event that can be referred to in future enquiries so that the actual tender exercise is limited to a commercial phase. Depending on internal governance processes of each purchaser, this can translate into 4-6 months reduction in tendering timescales although a significant effort is required on the very first tender event to build the mentioned catalogue. Where there are significant changes in purchaser technical specification or manufacturer design practices, the whole process would need to be repeated. Figure 3 illustrates the basic stages of a standard transformer design concept-based procurement process. This approach is also very effective in urgent purchases type scenarios to replace faulted transformers where strategic spare units are not available. Manufacturer

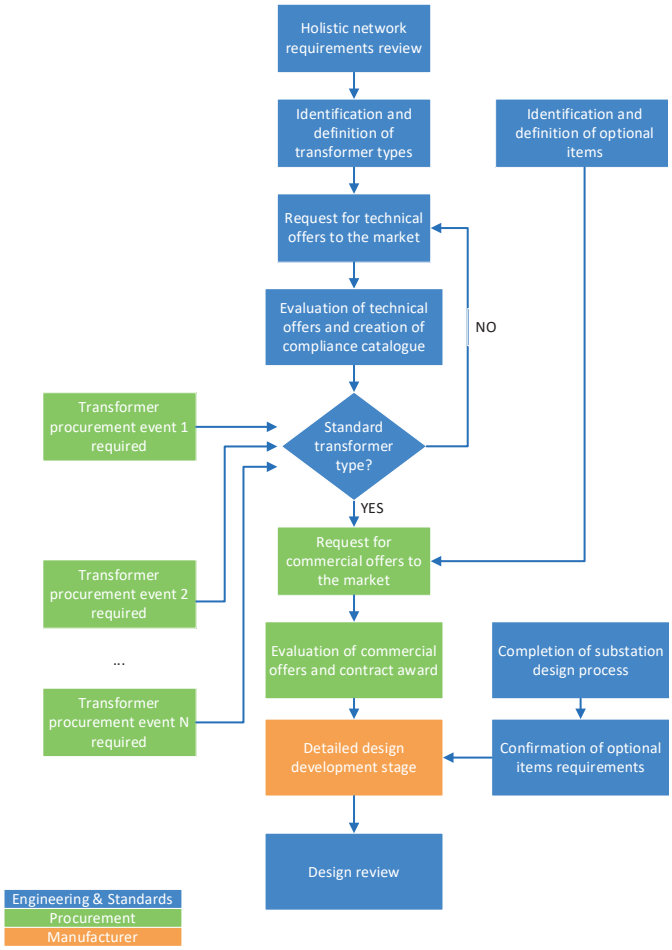

Fig. 3. Simplified flowchart of a standard transformer design concept based procurement process

III. Adaptative Strategies on Commercial Areas

A. Contracting Model

The standardisation exercise described in the previous sections, alongside establishing a closer relationship with other key stakeholders in the business, in order to understand longer-term requirements, and the de-coupling of technical and commercial tender phases, have all assisted in developing SP Energy Networks contracting model and tendering processes to adjust to the current market conditions.

Competition is an underlying principle in procurement policy, and widely acknowledged to be a key enabler of value for money. It helps the purchaser to secure the goods and services it requires at the right price and quality and is the best way of demonstrating probity in the award. The practice of acting ethically and fairly to all suppliers and stakeholders, allows the purchaser to comply to the procurement processes according to the tender requirements, set criteria, standards, or principles and to ensure adherence with purchaser's policies and rules.

The tendering process is a structured process, which is fair and transparent and includes a defined selection process with clear award criteria. By de-coupling technical and commercial tender phases, it is possible to simplify the award criteria to purchase price, or other defined lifetime cost calculation mechanisms, i.e. total cost of ownership (TCO) which accounts for losses capitalisation during the lifetime of the asset. This is achievable as technical evaluation of the offers would have been already performed in the previous phase of the process and reduces the formal tender event to a commercial phase only.

This contracting model makes the process repetitive, and consequently provides the purchaser with a current and up to date view of market conditions in price, lead-times, and capacity. The purchasers may have limited influence on market conditions for this type of equipment, but it is extremely important for the manufacturers to understand the purchasers and have the flexibility to adapt accordingly. This repetitive process also makes possible to tender multiple times in short periods of time and have a high percentage of comparability to previous prices paid. This provides an important regular insight to market changes in price, lead-times, and capacity, which can lead to changes in tendering strategies i.e., tendering earlier or later and budget forecasting.

In the current market conditions, it is extremely difficult to contract on fixed price basis as used to be the traditional approach within SP Energy Networks. This is primarily due to volatility of raw materials prices and other associated costs to the manufacturing process, further compounded by extended lead times and earlier placements of orders. Through negotiation with manufacturers, the implementation of price adjustment formulas (CPA), incorporating not only traditional raw materials in transformer manufacturing (magnetic steel, conductor material, etc.), but also some other volatile costs (insulating liquid, transport, etc.), resulted in a better distribution of uncertainties, and optimization of risk provisions, with the overall outcome of a more reasonable unit price for the purchaser and a lowest financial risk to the manufacturer. However, as it may be difficult to predict the point in time at which all these factors stabilise, it may be advisable to allow manufacturers to offer multiple pricing (i.e. fixed vs. CPA) with their associated conditions for the purchaser to evaluate.

Flexible contracting model makes possible to spread purchasing decisions over time and aligned to an agreed strategy to take advantage of movements in the market. This involves adapting to changing requirements, collaborating with manufacturers and stakeholders based on feedback and learning.

In conjunction with the tendering process, the purchaser should consistently monitor and asses the bidders on aspects such as financial risk, audit & insurance, management systems, accident rates, human rights, equality, diversity, sustainability, ethics and governance.

Additionally, a number of aspects following award decision shall be also considered as key enablers to facilitate an efficient and agile contract award process. A stable supplier base together with consistent set of legal and commercial requirements make possible to pre-agree a number of elements that, despite requiring final confirmation on each individual award, will fast-track these last stages

Jose Quintana, Wilson Smith, Mateja Cepin, New Transformer Procurement Concepts in Times of High Uncertainty and Market Instability, Journal of Energy, vol. 73 Number 1 (2024), 3–7
https://doi.org/10.37798/2024731504

of the procurement process. This typically includes: total cost of ownership calculator; terms & conditions; security provisions; and escalation formulas (CPA) and indices. This also represents a key part of the process to stay ahead of the supply curve and deal with short proposal validity periods.

All the factors detailed in this section assist in completing the commercial aspect of a tendering process in a period of 4 - 6 weeks, with notification and award taking a further 4 - 6 weeks. This significantly reduces the historical tendering time within SP Energy Networks and enables the business to commit to the manufacturers quickly securing the required manufacturing slots and, in instances, the benefit of fixed pricing against variable pricing. As illustration, with this process already set up, in early 2023 SP Energy Networks managed to purchase eleven large power transformers (132kV and above) on a full competitive tender process in 8 weeks from issuing the enquiry to the market to obtaining internal authorization for award. In the past, with a traditional approach, this would have taken 6- 8 months assuming all substation design processes were completed to allow the tender to be initiated.

This significant reduction in time is also an advantage to manufacturers, as it closes tendering events very quickly with feedback offered on their proposal if unsuccessful for preparation in advance of the next tendering process.

IV. Conclusions

Procurement strategies in the area of power transformers should be flexible enough to acknowledge and adapt to varying market conditions and ensure the most optimum solution, from technical, commercial and project delivery perspectives, is reached in each individual tender event. In the current environment of market saturation and various supply chain issues, it is particularly important to simplify and streamline procurement processes and improve engagement with key stakeholders within the purchaser business to clearly define long-term purchasing plans.

In achieving the above, decisions and strategies on the technical area play a key part as standardisation of transformer types, decoupling of substation design development and power transformer procurement, and simplification of design variants and site-specific requirements contributes significantly to reduce tender timescales which assists to offset the increasing lead times currently offered by the market. To mitigate against the possible rigidity of this approach, mechanisms can be built into the process to account for the particularities associated with each individual substation layout and/or installation considerations.

The standard transformer design concept defined in this paper has been proven to be a successful strategy within SP Energy Networks to be able to place power transformer orders early enough to ensure the business capital investment plans can be delivered as per agreed programmes; and pricing uncertainties and associated commercial risks are reasonably shared between manufacturer and purchaser. This approach and its repeatability, together with a stable supplier base, further assists to shorten tender timescales in multiple tender event situations and reduce resource dedication requirements, not only at tender stage, but potentially at subsequent equipment assessment and substation development following contract award.

Jose Quintana, Wilson Smith, Mateja Cepin, New Transformer Procurement Concepts in Times of High Uncertainty and Market Instability, Journal of Energy, vol. 73 Number 1 (2024), 3–7
https://doi.org/10.37798/2024731504

Journal of Energy

VOLUME 73 Number 1 | 2024

journal homepage: http://journalofenergy.com/

Hybrid Analytical-FEM Approach for Power Transformer Transient Analysis

Bruno Jurišić, Zvonimir Jurković, Tomislav Župan, Mladen Marković

***Summary* — The paper describes a high-frequency model for transient calculation in transformer windings with segmentation on a turn level. The windings are represented by lumped RLC parameters given by the analytical approach, whereas the model is solved in the time domain. The accuracy of the analytical calculation is improved with correction factors obtained with a set of numerical calculations. The presented model is verified by measurements on the example of power transformer disc winding.**

***Keywords* — transformer, transients, high-frequency model, inductance, capacitance.**

I. Introduction

One of the key factors influencing the reliability and lifespan of power transformers is the quality and proper dimensioning of their insulation. In addition to nominal voltages, power transformers are susceptible to overvoltages resulting from lightning strikes or switching operations. During such events, the dielectric stress in insulation can be significantly increased. A properly designed insulation must withstand the impulse voltages according to international standards [1]. To dimension insulation properly during the insulation design phase, overvoltages and voltages inside transformer have to be calculated using suitable models.

Internal transient overvoltages within power transformers are typically calculated using white-box high-frequency models [2]. In these models, the windings are represented by lumped RLC parameters, which are calculated using analytical or numerical methods [3]. After modeling the winding using RLC parameters, i.e. electrical circuit, the resulting system of Kirchhoff equations is solved, either in the time or frequency domain. In the high-frequency model, the windings are segmented into elements, which can range from the entire winding down to the level of individual discs or turns. In the proposed model, windings are modeled at the turn level, which increases the accuracy of the model and enables direct calculation of detailed distribution of voltage within the winding. According to the reference [4], the valid frequency range of the high-frequency model is related to the length of the segments. The length of the segment should be at least four times smaller than the wavelength that corresponds to the highest frequency. The radius of the power transformer winding is typically up to one meter. Therefore, the valid frequency range of the proposed model is approximately 10 MHz.

The calculation of RLC parameters is presented in Section II. The segmentation of the windings on a turn level implies the calculation of inductances (self and mutual), resistances and capacitances for each winding turn. There can be over thousands of turns in transformer windings, so methods that enable fast calculation are used. Capacitances are calculated using the analytical formulas and correction factors based on numerous 2D FEM calculations [5]. The inductances are calculated using the semi-analytical approach, based on work presented in papers [6-7]. The expressions given in these papers do not include infinite series [8], complex mathematical functions such as Bessel, Struve, and Legendre functions [9-10], or elliptic integrals [11]. Numerical integration, required in papers [6-7], is avoided by introducing the approximation of integral. The resistances, representing losses caused by skin and proximity effect, are calculated using the simple analytical formulas that can be found in the literature [12-13]. The model for magnetic field calculation, required for proximity loss calculation, is derived from Biot-Savart law. To validate the proposed model, a comparison is made against measurements conducted on the power transformer winding model, with details of the measurement setup shown in Section III and results presented in Section IV.

II. Transformer Model

The calculation of RLC parameters is presented in this section. The inductances and resistances are calculated using an air-core model that ignores the permeable core. This assumption is valid for calculation of high frequency overvoltages [4]. The capacitances are calculated using simple analytical formulas for plate capacitors and correction factors based on numerous 2D FEM calculations. After modeling the winding using the lumped RLC parameters, the nodal analysis in time domain is performed using the well-established Dommel's method [14].

A. Capacitance

The capacitances between winding turns are calculated using the approach presented in reference [5]. The turn-to-turn capacitances are calculated between adjacent turns with significant capacitive coupling using simple analytical formulas for plate and cylindrical capacitors. Above-mentioned analytical formulas assume simplified geometry and homogeneous electric field which lead to inaccurate results. Therefore, correction factors, based on numerous 2D FEM calculations, are introduced to improve accuracy.

Permittivities of oil, paper and spacers are considered using the equivalent permittivity. It is important to emphasize that influence

(Corresponding author: Zvonimir Jurković)

Bruno Jurišić, Zvonimir Jurković and Tomislav Župan are with the Končar - Electrical Engineering Institute Ltd., Zagreb, Croatia (e-mails: bjurisic@koncar-institut.hr, zjurkovic@koncar-institut.hr, tzupan@koncar-institut.hr)

Mladen Marković is with the Končar – Distribution and Special Transformers Inc., Zagreb, Croatia (e-mail: Mladen.Markovic@koncar-dst.hr)

Bruno Jurišić, Zvonimir Jurković, Tomislav Župan, Mladen Marković, Hybrid Analytical-FEM Approach for Power Transformer Transient Analysis, Journal of Energy, vol. 73 Number 1 (2024), 8–13
https://doi.org/10.37798/2024731512

of additional materials inside transformer winding, such as spacers, on overvoltage waveforms is not negligible.

B. Inductance

The mutual inductance of two coaxial coils with rectangular cross-sections can be calculated as a linked flux in one coil, whereas there is a current of one ampere in the other coil (source of magnetic flux). The linked flux can be calculated from vector magnetic potential using the expression:

$$\phi = \oint \boldsymbol{A} d\boldsymbol{l}\,, \tag{1}$$

whereas the vector magnetic potential is related to the source current by integral of Green's function for vector magnetic potential:

$$\boldsymbol{A}(\boldsymbol{r}) = \frac{\mu_0}{4\pi} \int \frac{\boldsymbol{J}(\boldsymbol{r}')}{|\boldsymbol{r} - \boldsymbol{r}'|} d^3\,\boldsymbol{r}' \tag{2}$$

The expression (2) can be applied to the axisymmetric geometry shown in Fig. 1. The current density $\boldsymbol{J} = \frac{1A}{S_1}$ ($S_1 = (r_2 - r_1)(z_2 - z_1)$) is cross-section of first coil) inside first coil is integrated with respect to variables r, z, and φ to get the vector magnetic potential inside the region of the second coil. The vector magnetic potential inside the second coil is integrated with respect to variables R and Z (due to axisymmetric geometry, integration with respect to φ comes down to multiplication by 2π) and divided by cross-section of other coil $S_2 = (r_4 - r_3)(z_4 - z_3)$ to get the flux linkage of second coil, i.e. the mutual inductance between first and second coil. By combining the expressions (1) and (2), and the definition that the mutual inductance is equal to fluxed linked in one coil, whereas the current of one ampere is in the other coil, the following expression is obtained:

$$L_{12} = \frac{\mu_0}{S_1 S_2} \int Q(r, R, z, Z, \varphi) dr dR dz dZ d\varphi \tag{3}$$

where function $Q(r,R,z,Z,\varphi)$, for considered geometry, is given as

$$Q(r, R, z, Z, \varphi) = \frac{rR\cos(\varphi)}{\sqrt{r^2 + R^2 - 2rR\cos(\varphi) + (z - Z)^2}} \tag{4}$$

In references [6-7], integral (3) is solved analytically with respect to variables *r, R, z,* and *Z*. That function's arguments are coils' geometry parameters $r_1, r_2, r_3, r_4, z_1, z_2, z_3, z_4$, and azimuthal variable φ. That function is denoted by G, whereas the arguments, except for the azimuthal variable φ, are left out for the sake of conciseness.

The goal is to obtain the approximation of integral:

$$L_{12} = \frac{\mu_0}{S_1 S_2} \int_{\varphi=0}^{\pi} G(\varphi) d\varphi \tag{5}$$

in closed-form to enable calculation of L matrix on turn level in acceptable time range. Function $G(\varphi)$ is equal to integral of $Q(r, R, z, Z, \varphi)$ with respect to variables *r, R, z,* and *Z*. Detailed derivation of function $G(\varphi)$ is given in [6-7].

A G function has a characteristic shape with the following properties:

- The function has a maximum at point $\varphi=0$ (from now on denoted as G_0) and minimum at point $\varphi=\pi$ (from now on denoted as G_π).
- The function is monotonically decreasing.
- Value of G function at point $\varphi = \frac{\pi}{2}$ is equal to zero.
- Absolute value of G_π is smaller than G_0.

Examples of G function, for different geometries of coils, are shown in Fig. 2. Physically, G function with narrow shape of positive part of the function and small ratio $\frac{G_\pi}{G_0}$ corresponds to the coils that are close to each other. By increasing the distance between coils, the shape of G function is closer to the cosine. The approximation of the integral of the G function assumes that the integral value can be correlated with the ratio $\frac{G_\pi}{G_0}$.

To get the approximation of integral (5), numerous calculations of G function's integral, using expressions from paper [7], were performed. Then, integral value is expressed using the rational functions, where the coefficients of the numerator and denominator polynomials were obtained using the least squares method:

$$\int_{\varphi=0}^{\pi} G(\varphi) d\varphi \approx G_0 \left[\frac{0.008618 \left(\frac{G_\pi}{G_0}\right)^3 + 9.711 \left(\frac{G_\pi}{G_0}\right)^2 + 159.6 \frac{G_\pi}{G_0} + 75.62}{\left(\frac{G_\pi}{G_0}\right)^3 + 35.03 \left(\frac{G_\pi}{G_0}\right)^2 + 131.3 \frac{G_\pi}{G_0} + 77.74} - \frac{1.07 \frac{G_\pi}{G_0} - 0.5949}{\left(\frac{G_\pi}{G_0}\right)^2 - 0.5201 \frac{G_\pi}{G_0} - 0.002404} \right]. \tag{6}$$

Above-mentioned expressions can be used to calculate the self-inductance. In that case, geometrical parameters are $r_3 = r_1 + \Delta$, $r_4 = r_2 + \Delta$, $z_3 = z_1 + \Delta$, and $z_4 = z_2 + \Delta$. Small displacement Δ is aded to avoid singularities, which are explained in papers [6-7]. In this paper, that displacement is $\Delta = 10^{-6}$.

Expressions for $G0$ and $G\pi$ are given in papers [6-7].

C. Resistance

The resistances in the proposed model include DC resistance, and AC resistances that represent losses due to skin and proximity effects. The resistance per unit length that takes skin effect into account is calculated using the expression [13]

$$R'_{skin} = \frac{1}{4\sigma(h + w)^2} \left[\frac{h}{\delta} \frac{\sinh\left(2\frac{w}{\delta}\right) + \sin\left(2\frac{w}{\delta}\right)}{\cosh\left(2\frac{w}{\delta}\right) + \cos\left(2\frac{w}{\delta}\right)} + \frac{w}{\delta} \frac{\sinh\left(2\frac{h}{\delta}\right) + \sin\left(2\frac{h}{\delta}\right)}{\cosh\left(2\frac{h}{\delta}\right) + \cos\left(2\frac{h}{\delta}\right)} + 2 \right] \tag{7}$$

where w and h are width and height of the conductor, respectively. If the conductor consists of more separately insulated wires (e.g. continuously transposed conductor), resistance for each wire is calculated separately. The parameter σ is the electrical conductivity of conductor, and the parameter $\delta = \sqrt{\frac{1}{\pi f \mu \sigma}}$ is the skin depth of conductor. R matrix is calculated at arbitrarily chosen frequency f=10 kHz..

To calculate the losses due to proximity effect, magnetic field at the position of another coil (r_0, z_0) must be calculated. The geometry of windings is simplified to get simple mathematical expressions. The permeable core is neglected and the geometry of winding is assumed to be planar (see Fig. 3). Expressions for magnetic field are derived from Biot-Savart law:

$$\boldsymbol{B}(\boldsymbol{r}) = \frac{\mu_0}{4\pi} \int \frac{I d\boldsymbol{l} \times \boldsymbol{r}'}{|\boldsymbol{r}'|^3} \tag{8}$$

For the geometry shown in Fig 3 (infinitely long coil of rectangular cross-section with current of one ampere), Biot-Savart (8) can be written as:

$$B(r_0, z_0) = \frac{\mu_0}{4\pi (r_2 - r_1)(z_2 - z_1)} \int_{l=-\infty}^{\infty} \int_{r_1}^{r_2} \int_{z_1}^{z_2} \frac{(z_0 - z)\vec{a_r} - (r_0 - r)\vec{a_z}}{\sqrt{l^2 + (r_0 - r)^2 + (z_0 - z)^2}^3} dl\, dr\, dz. \tag{9}$$

Bruno Jurišić, Zvonimir Jurković, Tomislav Župan, Mladen Marković, Hybrid Analytical-FEM Approach for Power Transformer Transient Analysis, Journal of Energy, vol. 73 Number 1 (2024), 8–13
https://doi.org/10.37798/2024731512

By solving the integral (9), and components of the magnetic field are obtained:

$$B_r = k\left[\left((r_0 - r)ln((r_0 - r)^2 + (z_0 - z)^2) + 2(z_0 - z)\tan^{-1}\left(\frac{r_0 - r}{z_0 - z}\right)\right)\right.$$
$$\left. + \left((r_0 + r)ln((r_0 + r)^2 + (z_0 - z)^2) + 2(z_0 - z)\tan^{-1}\left(\frac{r_0 + r}{z_0 - z}\right)\right)\right]\Big|_{r=r_1}^{r_2}\Big|_{z=z_1}^{z_2}, \quad (10)$$

$$B_z = k\left[\left((z_0 - z)ln((z_0 - z)^2 + (r_0 - r)^2) + 2(r_0 - r)\tan^{-1}\left(\frac{z_0 - z}{r_0 - r}\right)\right)\right.$$
$$\left. + \left((z_0 - z)ln((z_0 - z)^2 + (r_0 + r)^2) + 2(r_0 + r)\tan^{-1}\left(\frac{z_0 - z}{r_0 + r}\right)\right) + 4z\right]\Big|_{r=r_1}^{r_2}\Big|_{z=z_1}^{z_2}, \quad (11)$$

$$k = \frac{\mu_0}{4\pi(r_2 - r_1)(z_2 - z_1)}. \quad (12)$$

After the calculation of magnetic field, the losses (equal to resistance since current in first coil is one ampere) due to proximity effect per unit length are calculated separately for each component of the magnetic field. For that purpose, simple, well-known expressions for eddy-current losses (per unit volume) in infinite planar plate of thickness t and conductivity σ (page 154 in [12]) are used:

$$p = \frac{(2\pi f)^2 B^2 t^2 \sigma}{24} \quad (13)$$

By combining the expressions (10-14), the resistance per unit length is calculated as:

$$R'_{proximitty} = \frac{\sigma\pi^2 f^2 \left(B_r{}^2 h^3 w + B_z{}^2 w^3 h\right)}{6} \quad (14)$$

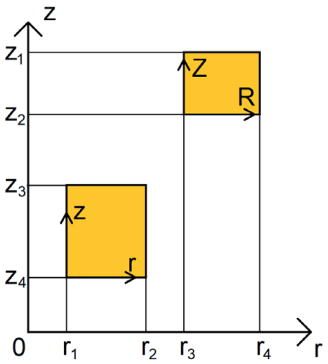

Fig. 1. The geometry of two circular coaxial coils with rectangular cross-sections

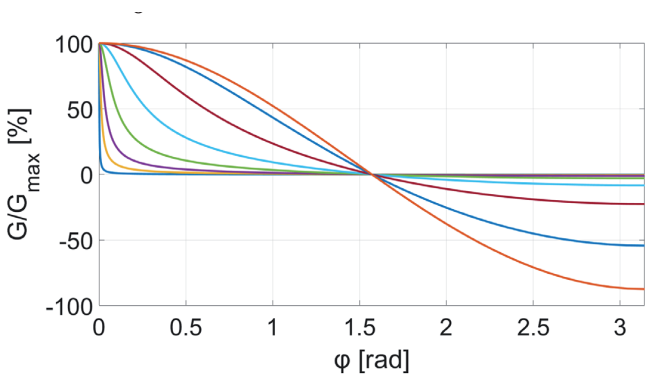

Fig. 2. The examples of G function for different coil's geometries

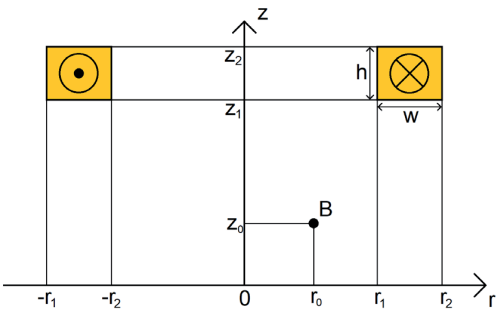

Fig. 3. The geometry of model for calculation of magnetic field

III. Measurements on Power Transformer Winding Model

To verify the proposed methodology, the overvoltages are measured on the power transformer winding model (see Fig. 4). The model includes two axially stacked disc windings that are pressed between two steel plates, with no tank or oil. The upper winding has 48 discs and 9 conductors in disc, whereas the bottom winding has 48 discs and 10 conductors in disc. The standard impulse test wave 1.2/50 μs is generated using the surge generator *Haefely type 481*. To enable measurement of voltage along the winding, insulation is removed and copper terminals are soldered in 48 places. Then, voltage waveforms at these terminals are measured using the oscilloscope *Tektronix DPO 4054* and measuring probes. The measurement setup is illustrated in Fig. 5.

Fig. 4. The winding model

Bruno Jurišić, Zvonimir Jurković, Tomislav Župan, Mladen Marković, Hybrid Analytical-FEM Approach for Power Transformer Transient Analysis, Journal of Energy, vol. 73 Number 1 (2024), 8–13
https://doi.org/10.37798/2024731512

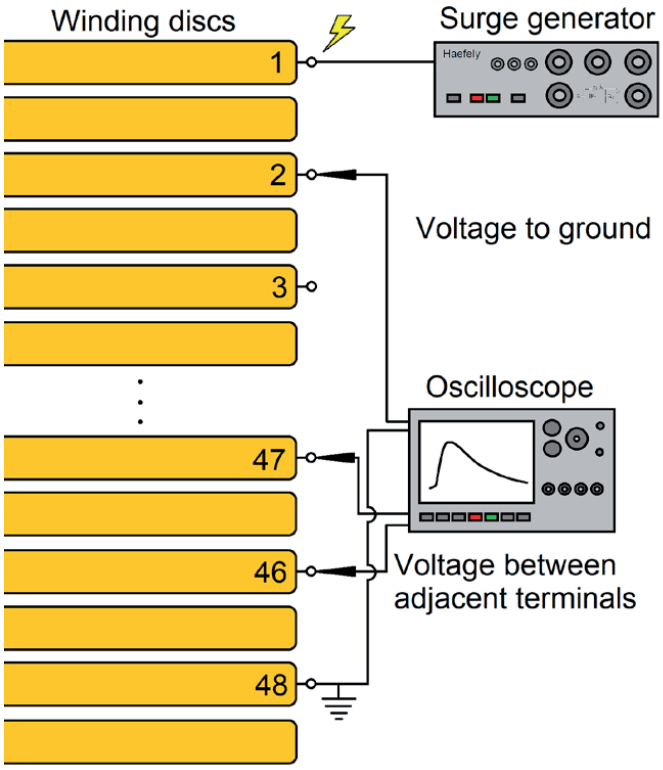

Fig. 5. The measurement setup

IV. Mathematical Model Results

The overvoltages along the winding model are calculated using the methodology proposed in Section II. The results are compared against the measurements. Then, the visualization of voltages in the winding, using color mapping, is presented.

A. Model verification

The calculated voltage waveforms at three terminals and distribution of maximum voltages to ground along the winding are compared against the measurements. The comparison is shown in Fig. 6.

The error for maximum values of voltages, shown in Fig. 6, are given in Table I.

Table I.

Relative Errors For Maximum Values of Voltages

	Error [%]
Terminal 7 waveform	-1.2
Terminal 17 waveform	-4.6
Terminal 27 waveform	1.7
Distribution along winding	-3.2

B. Visualization of voltages in the winding

The proposed model enables the calculation of voltage waveforms for every single turn. Such detailed results can be represented in various ways, numerically and visually. Spatial distribution of voltage can be represented visually for the entire winding using color mapping. Maximum voltages to ground and voltages between adjacent turns (radially, axially and diagonally) of interleaved winding with radial and axial channel are shown in Fig. 7. Except maximum values, voltage values can be shown for every time step. By taking series of images with voltage values for every time step, animation can be generated that shows behavior of voltage in space and time (for example, propagation and reflections of transient wave can be shown).

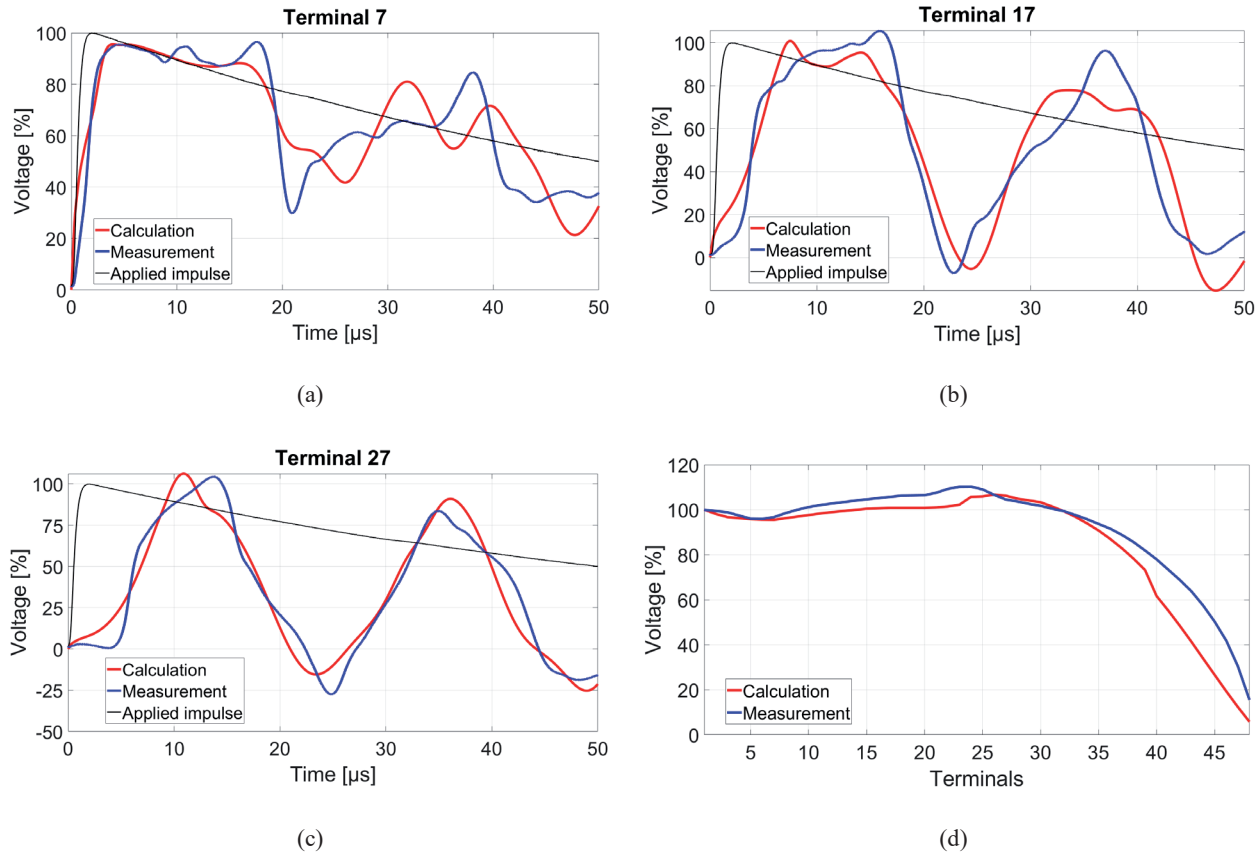

Fig. 6. The voltage waveforms at terminals 7 (a), 17 (b), 27 (c), and distribution of maximum voltages to ground along the winding (d)

Bruno Jurišić, Zvonimir Jurković, Tomislav Župan, Mladen Marković, Hybrid Analytical-FEM Approach for Power Transformer Transient Analysis, Journal of Energy, vol. 73 Number 1 (2024), 8–13
https://doi.org/10.37798/2024731512

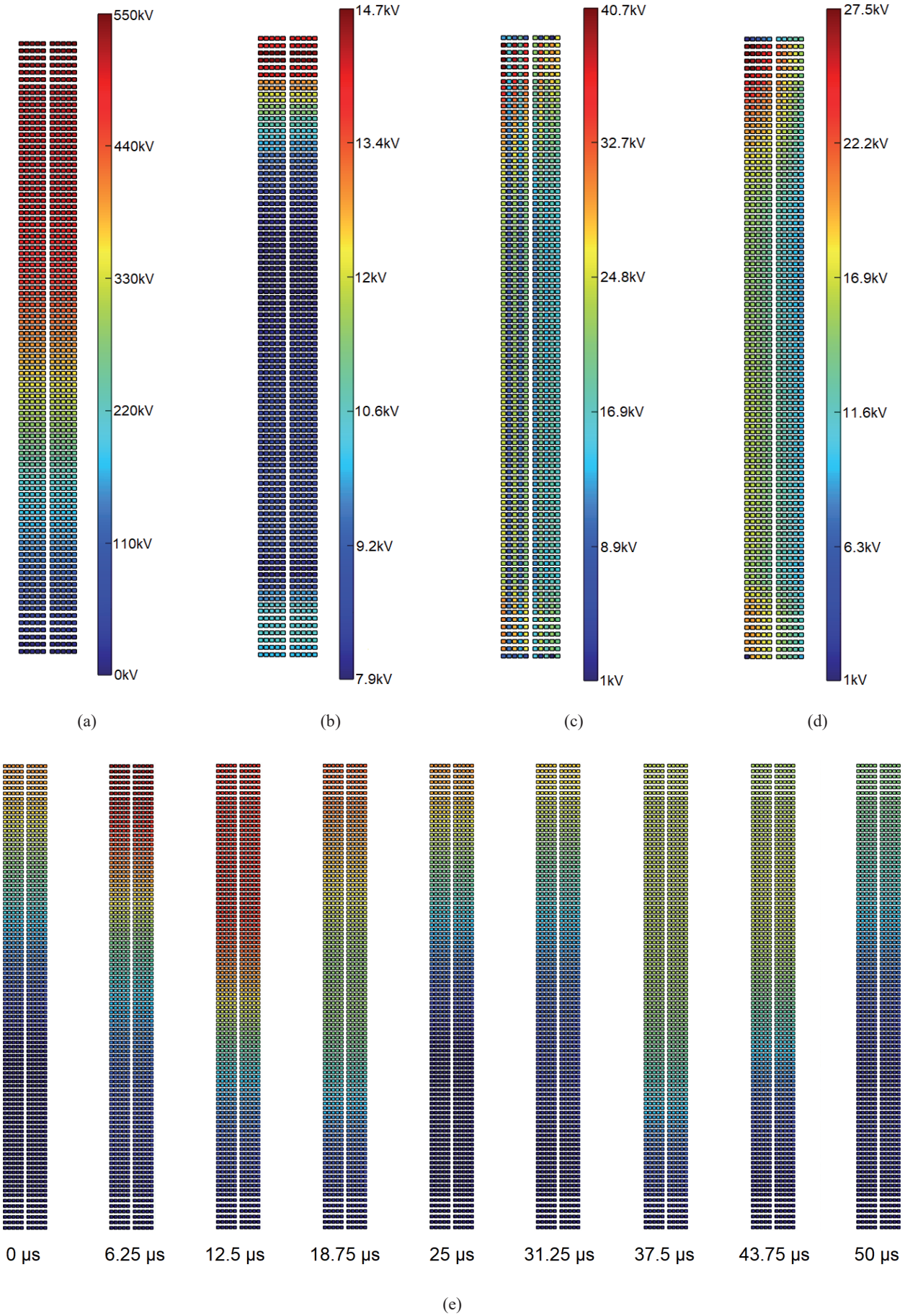

Fig. 7. The representation of maximum voltages to ground (a), and between radially (b), axially (c) and diagonally (d) adjacent turns. Propagation of transient wave is shown by series of images with instantaneous values of voltage (e)

Bruno Jurišić, Zvonimir Jurković, Tomislav Župan, Mladen Marković, Hybrid Analytical-FEM Approach for Power Transformer Transient Analysis, Journal of Energy, vol. 73 Number 1 (2024), 8–13
https://doi.org/10.37798/2024731512

V. Conclusion

The methodology for calculation of transient overvoltages in a power transformer is presented in the paper. The transformer winding is modeled down to the level of turn, using lumped RLC parameters. The model is solved in time domain using Dommel's method. The capacitances are calculated using simple analytical models and correction factors based on the 2D FEM. The inductances and resistances are calculated using analytical models that neglect the permeable core, which is valid when calculating high frequency transients. The proposed methodology enables fast calculations even with complicated transformer winding geometries with thousands of turns. The calculation of RLC parameters is in a time range of seconds, whereas the calculation in the time domain is in a time range of tens of seconds. That makes the proposed methodology suitable for application in the transformer design process.

The mathematical expressions for the calculation of inductances are derived using the Green's function for vector magnetic potential. To derive the expressions, multiple integral with respect to five variables must be solved. In the existing literature, integral is solved with respect to four variables, whereas numerical integration with respect to the fifth variable is necessary. To avoid numerical integration, approximation of the unsolved integral is introduced. The resistances are calculated using simple analytical expressions from the existing literature. However, the model for calculation of the magnetic field is derived from the Biot-Savart law with assumption of planar geometry of windings. The closed-form expressions for inductances and resistances, with no need for numerical integration, allow very fast calculations.

The measurements of overvoltage distribution on the experimental winding model are done to verify the proposed approach. The comparison between calculation and measurement results has shown good accuracy of the proposed model, as in the worst case the amplitude error is less than five percent. The possibility of detailed visualization of voltage in the winding is presented. Except standard representation of results, such as numerical data or 2D plots of waveforms, detailed visualization of voltages in the windings or between the windings can be a very helpful tool for power transformer design engineers.

References

[1] "IEC 60060–1", High-voltage test techniques Part 1: General definitions and test requirements, 2010

[2] E. E. Mombello, G. A. Díaz Flórez, "An improved high frequency white-box lossy transformer model for the calculation of power systems electromagnetic transients," in Electric Power Systems Research, vol. 190, Jan. 2021, doi: 10.1016/j.epsr.2020.106838.

[3] T. Župan, B. Trkulja, R. Obrist, T. Franz, B. Cranganu-Cretu and J. Smajic, »Transformer Windings' RLC Parameters Calculation and Lightning Impulse Voltage Distribution Simulation,« in IEEE Transactions on Magnetics, vol. 52, no. 3, pp. 1-4, March 2016, Art no. 8400204, doi: 10.1109/TMAG.2015.2481004.

[4] CIGRE JWG A2/C4.52., "High Frequency Transformer and Reactor Models for Network Studies – Part A: White-Box Models", CIGRE, technical brochure, 2023.

[5] Z. Jurković, B. Jurišić, M. Marković and T. Župan, »Improved Analytical Calculation of Winding Capacitance Using Correction Factors,« *2022 7th International Advanced Research Workshop on Transformers (ARWtr)*, Baiona, Spain, 2022, pp. 30-35, doi: 10.23919/ARWtr54586.2022.9959895.

[6] T. Župan, Ž. Štih and B. Trkulja, »Fast and Precise Method for Inductance Calculation of Coaxial Circular Coils With Rectangular Cross Section Using the One-Dimensional Integration of Elementary Functions Applicable to Superconducting Magnets,« in *IEEE Transactions on Applied Superconductivity*, vol. 24, no. 2, pp. 81-89, April 2014, Art no. 4901309, doi: 10.1109/TASC.2014.2301765.

[7] S. Liang and Y. Fang, »Analysis of Inductance Calculation of Coaxial Circular Coils With Rectangular Cross Section Using Inverse Hyperbolic Functions,« in *IEEE Transactions on Applied Superconductivity*, vol. 25, no. 4, pp. 1-9, Aug. 2015, Art no. 4901209, doi: 10.1109/TASC.2015.2427353.

[8] Dwight, H., Chen, S., "An extension of a maxwell mutual-inductance formula to apply to thick solenoids", Journal of Applied Physics, Vol. 4, No. 9, 1933, str. 323–326.

[9] Conway, J. T., "Inductance calculations for circular coils of rectangular cross section and parallel axes using Bessel and Struve functions", Magnetics, IEEE Transactions on, Vol. 46, No. 1, 2010, str. 75–81.

[10] Hurley, W. G., Duffy, M. C., "Calculation of self and mutual impedances in planar magnetic structures", Magnetics, IEEE Transactions on, Vol. 31, No. 4, 1995, str. 2416–2422.

[11] Garrett, M. W., "Calculation of fields, forces, and mutual inductances of current systems by elliptic integrals", Journal of Applied Physics, Vol. 34, No. 9, 1963, str. 2567–2573.

[12] S. V. Kulkarni, »Transformer Engineering: Design, Technology and Diagnostics«, CRC Press., Second Edition, 2012.

[13] R. L. Stoll, *The Analysis of Eddy Currents*. Oxford: Oxford University Press, 1974.

[14] H. W. Dommel, »Digital Computer Solution of Electromagnetic Transients in Single-and Multiphase Networks,« in *IEEE Transactions on Power Apparatus and Systems*, vol. PAS-88, no. 4, pp. 388-399, April 1969, doi: 10.1109/TPAS.1969.292459.

Journal of Energy
VOLUME 73 Number 1 | 2024
journal homepage: http://journalofenergy.com/

Measurement Uncertainty in On-line Bushing Monitoring

Wiesław Gil, Wiktor Masłowski

***Summary* — The high voltage bushing on-line monitoring has been performed for many years to prevent unexpected rapid power network failures. Network unbalance correction, based on separate voltage phase measurement or phasor technique, effectively improves the measurements of bushing dielectric dissipation factor tgδ and capacitance factor C_1. The newly implemented monitoring units reveal that the uncertainty of station voltage measuring transformers manifest the greatest influence on the overall uncertainty budget, regardless of the measurement method.**

***Keywords* — Online bushing monitoring, power network unbalance, measuring uncertainty of isolation coefficients.**

I. High Voltage Bushing Monitoring

The properties of bushings are susceptible to gradual degradation caused by material aging accelerated by temperature changes, weather conditions, and disturbances occurring during power grid operation. These processes can lead to sudden failure of the bushing, resulting in, at least, a transformer shutdown. [1].

For many years a systematic assessment of the condition of the bushing has been carried out, based not only on the results of periodic tests and measurements, but also on online monitoring. This assessment involves the continuous values analysis and trends evaluation related to bushing dielectric loss coefficient tgδ and its capacitance C_1. These parameters are determined based on leakage current or voltage measured at the bushing's measure taps. Measuring systems, based on probes located in bushings' measuring sockets and monitoring modules, are installed to collect data and determine the insulation indicators mentioned above. Remote or local servers process and collect data over a long period of time, presenting the results through charts, tables, warnings and alarms.

In the oldest solutions from the last century, the leakage currents of bushings operating in three-phase autotransformers and transformer systems were summarized and the total leakage current was measured. [2]. After the year 2000, methods known as the relative methods were developed for online measurements of insulation indicators. These methods do not directly determine the insulation indexes, but specify changes relative to their initial values. A relative voltage method is one of such methods. Additionally, there are direct methods known, were the values of leakage currents or the parameters of the relevant voltage vectors are directly evaluated by phasors measurements.

(Corresponding author: Wiesław Gil)
Wiesław Gil and Wiktor Masłowski are with the MIKRONIKA, Poznań, Poland (e-mails: wieslaw.gil@mikronika.com.pl, wiktor.maslowski@mikronika.com.pl)

II. Relative Voltage Method

The relative voltage method [3] is based on the model shown in Fig. 1 and 2. The C_1 represents the so-called main bushing capacitance, which reflects the resultant capacitance of the cylindrical capacitors forming its core. The capacitance C_2 represents the capacitance between the measuring tap and the ground potential. A reference capacitor C_W is connected to the bushing's measuring tap by the use of special probe. Thus, a divider of phase voltage U is created to measure the V voltage.

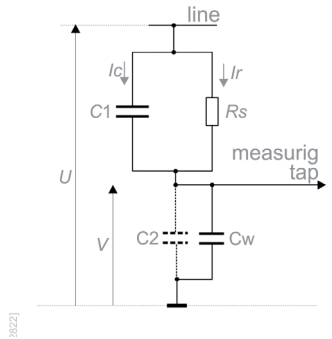

Fig. 1. Equivalent of the bushing with the capacitor Cw connected to the measuring tap

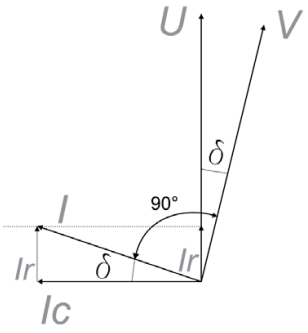

Fig. 2. Vector V displacement by δ angle

The C_W capacitance is selected to obtain V voltage of approximately 50V at the measuring tap. The capacitance C_2 can be neglected as it is several hundred times smaller than C_w. The resistance R_s represents the bushing's loss. The current I of the capacitor C_W is the sum of currents I_c and I_r. The tgδ value of the δ angle between

Wiesław Gil, Wiktor Masłowski, Measurement Uncertainty in On-line Bushing Monitoring, Journal of Energy, vol. 73 Number 1 (2024), 14–17
https://doi.org/10.37798/2024731509

the U and V voltage vectors, indicates the value of the bushing's dielectric dissipation factor. The described method is relative because it does not directly determine the insulation coefficient, but instead assesses their relative changes in relation to the initial values of C_{1p} and tgδ_p, which are obtained during off-line measurements or adopted according to the manufacturer's data.

During calibration, the C_W value is determined according to equation (1), for the actual phase voltage U_p and the measurements voltage V_p.

$$C_w = C_{1p}\left(\frac{U_p}{V_p} - 1\right) \tag{1}$$

Then, bushing capacity C_1 values are calculated according to the equation (2) in relation to the voltage changes on C_w.

$$C_1 = \frac{C_w}{\frac{U_p}{V_p} - 1} \tag{2}$$

If the tgδ_p value is known from off-line measurements, the current values and changes in the dielectric loss factor tgδ are determined relative to the initial tgδ_p value. If a change of dielectric properties, causing the change of the vector angle, occurs only in one phase A as shown in Fig. 2, then the value of tgδ_{AD} can be determined basing on the eq. (3).

$$\tan\delta_{AD} = [\tan(\delta_{AD} - \delta_{Ap}) + \text{arctg}\delta_{Ap}] \tag{3}$$

Where:

δ_{AD} – actual angle displacement of phase A bushing voltage

δ_{Ap} – initial angle displacement of phase A bushing voltage vector, based eg. on last bushing service measurements

In earlier applied solutions [3], the initial values of δ_{Ap}, δ_{Bp}, δ_{Cp} angles were determined for each phase basing on off-line tgδ_{Ap}, tgδ_{Bp} ,tgδ_{Cp} measurements, and the positions of the phase voltage vectors V_A, V_B, V_C were corrected, as depicted in Fig. 3. One of the voltages $V_{(A,B,C)}$ was chosen as the reference voltage, and the angular displacements of the other two vectors were measured in relation to it. Similar relationships were applied to the other phases. However, due to the unbalance of the power network, the position of the V_D vector fluctuates, as shown in Fig. 4.

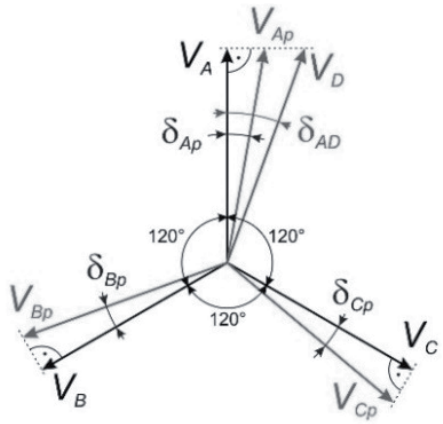

Fig. 3. Change in the positions of vectors VA, VB, VC, and the new position of vector VA due to increased dielectric losses

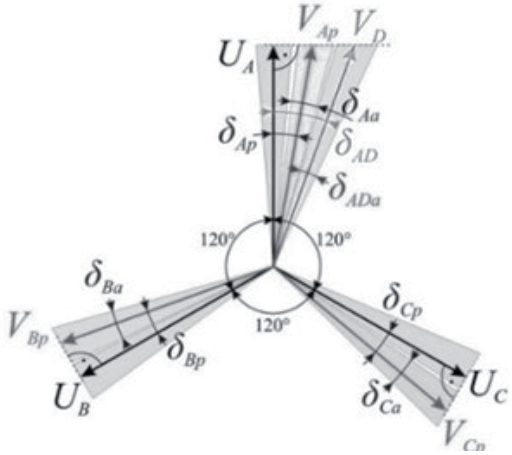

Fig. 4. Fluctuation in the positions of vectors VA, VB, VC, due to power network unbalance

Voltage unbalance is extremely important in "the depth "of the power network. For example, a momentary change of the δ angle between 10 and 30 minutes can result in a change in tgδ ranging from 0.3% to 0.8%. Such a change should be identified as exceeding the permissible tgδ value for OIP bushings. Even greater voltage unbalances than the above may occur in the power grid. As a result, the insulation coefficient measurements using the discussed method becomes very imprecise. This dysfunction was limited by the use of object learning algorithms, various filtration methods, and averaging results, even within 24 hours.

III. Monitoring with Power Network Unbalance Correction

In dozens of bushing monitoring systems operating in Poland, a power network unbalance correction has been introduced [4]. In the monitoring system, denoted as MM in Fig. 5, an independent converter was dedicated to measuring the voltage modules and phase angles at the substation voltage transformers. Having knowledge of modules and phase angles of voltage vectors measured at voltage transformers allows to determine the relative values of the corrected tgδ and C_1 coefficients for each bushing. Fig. 6 illustrates the MM-F modification introduced in 2021 to the MM systems. This modification involves the direct measurement of voltage vectors from voltage transformers in a single device, including measurements of voltage vectors from bushing measuring probes. All voltages are sampled synchronously. In the modified method, the phasors of the voltages measured at the measuring taps are determined every second in relation to the voltages from the station voltage transformers.

The capacitances C_1 of individual bushings in the modified system (MM-F) are determined in analogously to the unbalance correction method (MM). However, the vector modules and their angles are synchronously determined for the bushings and transformers HV and the LV line voltages. The modification removes additional errors in the angle and amplitude measurements caused by the lack of synchronization of sampling between the calculation module and the additional converter.

Wiesław Gil, Wiktor Masłowski, Measurement Uncertainty in On-line Bushing Monitoring, Journal of Energy, vol. 73 Number 1 (2024), 14–17
https://doi.org/10.37798/2024731509

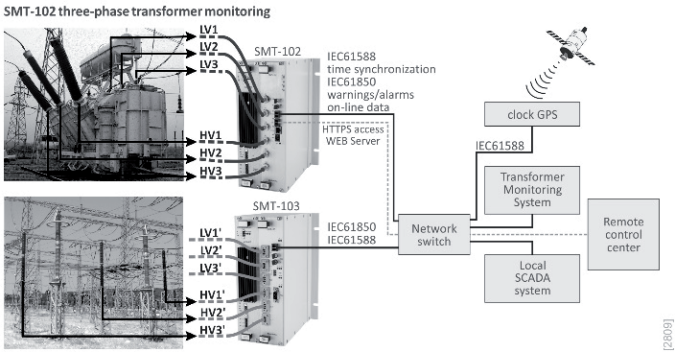

Fig. 5. Bushing monitoring measurements based on power network unbalance correction (MM)

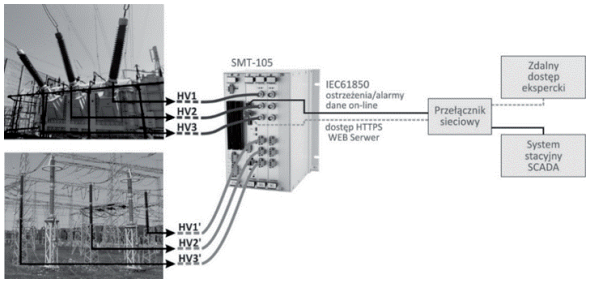

Fig. 6. Modified measuring device (MM-F)

IV. Factors Influencing Measurement Uncertainity

The determined values of C_1, tgδ and their changes over specific periods of time are compared to the criteria values established to inform about any occurring irregularities. It is important to identify the factors that influence the uncertainty of the conducted measurements, because it affects the reliability of the indicators, consequently, the usefulness of the installed bushing monitoring.

The measuring module properties are determined by the resolution and linearity of the measurement inputs, the temperature drift of the used components and the system's resistance to electromagnetic interferences. These factors influence the measurements on the basis of which the insulation coefficients are calculated. During laboratory tests of MM and MM-F units, the standard uncertainty of voltage measurement $u(U)$=0.01[V], and the measurement of the angle u(°)=0.002' was demonstrated.

The quality of the components in the measuring probe not only affects measurement stability, but also the reliability of the monitored transformer [5]. Failure of the measuring probe installed in the bushing measuring socket may lead to arcing, corrosion or other damage to the measuring tap, and in critical cases, it can lead to damage of the bushing. High quality polypropylene capacitors were applied in the probes to create the C_w capacitance. The average temperature drift of the probe was assessed to be 0.43nF/°C. It corresponds to a capacitance change C_1 of about 2pF/10°C. The change in the measured angle due to the temperature influence, converted to the value of tgδ, introduces the maximum standard uncertainty u(tgδ)=0.004 [%].

The uncertainty budget should include ***the bushing ratio uncertainty***. This uncertainty arises from the ratio variability between the phase voltage and the voltage measured at the test tap. The relevant characteristics were made in the transformer test room and the standard uncertainty of the voltage measured at the measuring terminal $u(V)$ was estimated in the range from 0.04 to 0.12 [%]. Lower uncertainties $u(V)$ were obtained after calibrating the system to compensate the permanent errors. When calibration was not carried out, then significantly higher uncertainties were observed.

The uncertainties of the station voltage transformers should be taken into account because the measurements obtained from these devices are used to evaluate and correct the phase unbalance. Therefore, based on the test protocols of class 0.2 station transformers, the uncertainties of angle and phase voltage measurements were determined for both calibrated and uncalibrated systems. These results are presented in Tab. 1. Based on the angle measurements uncertainty u(°), the maximum uncertainty equivalent contributed to the tgδ calculations was determined to be 0.01% for a calibrated system and 0.1% for an uncalibrated system, respectively. The uncertainty of the line voltage measurements was taken into account when calculating the combined uncertainty of the capacitance measurement $ud(C_1)$, using the total differential method.

Table I.

Uncertainity of Station Transformers

calibrated		uncalibrated	
u(°) [']	u(V) [%]	u(°) [']	u(V) [%]
0,15	0.01	3,4	0.1

V. Measurement Uncertainity of tg(δ)

For both presented systems, tgδ measurements were conducted on a laboratory stand, and the expected uncertainties in station conditions were estimated. The obtained results were then compared to the actual results at the power station. The measurements and the estimation uncertainty budget are presented in Tab. 2. When determining the extended uncertainty U(tgδ) in the laboratory, the standard deviations u(tgδ) resulting from the scattering of measurements and the equivalent uncertainty of the angle measurement u_Δ(tgδ) resulting from two independent measurements of the angle difference in two devices in the MM system and a single angle measurement in one device in the MM-F system were taken into account. The temperature of the probe was not specified in the budget because the measurements were conducted at a constant temperature. It was assumed that permanent errors were compensated for during the calibration of the laboratory system.

In the estimation for the station conditions, the standard measurement system uncertainty $u(tg\delta)$ was assumed based on measurements conducted in laboratory conditions. The equivalent u_Δ(tgδ) uncertainty resulting from the angle measurements on the station voltage transformers was taken into account - twice for the MM and once for the MM-F systems. The equivalent $u(T)$ resulting from the temperature influence on changes in the tgδ coefficient was also considered.

The complex standard uncertainty u_c(tgδ) in laboratory conditions is more than 100% higher in the MM system compared to the MM-F system, in which simultaneous sampling of voltages from measuring terminals and voltage transformers has been implemented. The estimation for station conditions shows an uncertainty of approximately 50% greater in the MM system than in the MM-F system. In the calibrated MM system, the complex standard uncertainties u_c(tgδ) estimated for station conditions are about 50% higher than in the MM-F system. The obtained results confirm the better measurement properties of the MM-F system. The lack of calibration increases multiple times the uncertainty in both the MM and MM-F systems.

Wiesław Gil, Wiktor Masłowski, Measurement Uncertainty in On-line Bushing Monitoring, Journal of Energy, vol. 73 Number 1 (2024), 14–17
https://doi.org/10.37798/2024731509

Tab. 2 also presents the uncertainty of *tgδ* measurements for the MM and MM-F systems, based on actual measurements conducted over a 15-day period performed at several power stations. In the MM system, the extended uncertainty $U(\mathrm{tg}\delta)$ ranges from 0.02 to 0.08. In the MM-F system, the maximum uncertainty is twice lower than in the MM system, which confirms its superior measurement properties. The actual maximum uncertainties are several times lower than the estimation for uncalibrated systems, in which constant errors have not been compensated. The minimum actual values of $U(\mathrm{tg}\delta)$ are analogous to the estimates for compensated systems.

TABLE II.

UNCERTAINITY BUDGET OF TG(Δ)[%] MEASUREMENTS

uncertainity tgδ [%]		laboratory		assessment for station condition				actual stations measurements	
				calibrated		not calibrated			
description	symbol	MM	MM-F	MM	MM-F	MM	MM-F	MM	MM-F
device dispersion	u(tgδ)	0,003	0,002	0,007	0,003	0,007	0,003	-	-
phase angle 1	u_{Δ}(tgδ)	0,004	0,002	0,005	0,005	0,099	0,099	-	-
phase angle 2	u_{Δ}(tgδ)	0,004	-	0,005	-	0,099	-	-	-
probe temperature	u(T)	-	-	0,004	0,004	0,004	0,004	-	-
complex	u_c(tgδ)	**0,007**	**0,003**	**0,01**	**0,007**	**0,14**	**0,1**	**-**	**-**
extended (95%)	U(tgδ)	**0,02**	**0,01**	**0,02**	**0,02**	**0,3**	**0,2**	**0,02-0,08**	**0,02-0,04**

VI. MEASUREMENT UNCERTAINITY OF CI

Similar to the tgδ measurements, C_1 measurements were performed in a laboratory. The expected uncertainties in station conditions were estimated and compared to the results obtained for real data. The measurements uncertainty budget and estimation are presented in Table 3. In the laboratory conditions, the $U(C_1)$ determination takes into account the standard deviation $u(C_1)$ resulting from measurements scattering, and the equivalent uncertainty $u(\Delta C_{1max})$ resulting from the calibration uncertainty of the measuring system. The uncertainty $u_d(C_1)$ resulting from the influence of the uncertainty of simulated line voltage measurements on the simulated voltages at the measuring terminal was considered. The probe temperature was not taken into account, as the measurements were conducted at a constant temperature. It was assumed that permanent errors were compensated during calibration.

TABLE III.

UNCERTAINITY BUDGET OF CI [PF] MEASUREMENTS

uncertainity C_1(pF)		laboratory		assessment for station condition				actual stations measurements	
				calibrated		not callibrated			
description	symbol	MM	MM-F	MM	MM-F	MM	MM-F	MM	MM-F
device dispersion	u(C_1)	0,01	0,01	0,17	0,15	0,17	0,15	-	-
calibration	u(ΔC_{1max})	0,04	0,03	-	-	-	-		
U/V relativ influence	u_d(C_1)	0,16	0,14	0,61	0,56	1,73	1,59	-	-
Probe temperature	u(T)	-	-	-	-	-	-	-	-
complex	u_c(C_1)	**0,17**	**0,15**	**0,63**	**0,58**	**1,74**	**1,6**	**-**	
extended (95%)	U(C_1)	**0,4**	**0,3**	**2**	**2**	**4**	**4**	**1,1-3,1**	**1,1-1,4**

In the estimation for station conditions, the standard uncertainty of the measurement system $u(C_1)$ was assumed based on laboratory measurements. The uncertainty $u_d(C_1)$ resulting from the influence of the uncertainty of measuring the actual phase voltage on the measuring tap voltage of the voltage transformers was also taken into account. The uncertainty resulting from the temperature $u(T)$ influence has not been taken into account. It was assumed that compensation is possible due to the observed linear nature of this influence, which causes an increase in the measured value of C_1 by approximately 2pF/10 °C increase in temperature.

Taking into account the monitoring module uncertainty under laboratory conditions, it was estimated that the extended uncertainty $U(C_1)$ of the capacitance measurement for a range of 400 to 500 pF in substation conditions will not exceed 2pF. If the measurement system is not calibrated, the voltage measurement uncertainty should be assumed as $u(U)$=0.1% of the measured value. For the uncertainty $u(V)$, which is 0.12% according to the tests, the expanded uncertainty of the capacitance measurement $U(C_1)$ reaches 4 pF. In the MM-F version, the maximum expanded uncertainties $U(C_1)$ determined based on the real measurements are more than twice as low in comparison to the MM system. This is due to the simultaneous sampling of the voltage at the measuring terminal and the phase voltage, which results in greater immunity to momentary voltage changes caused by short-term disturbances.

VII. CONCLUSIONS

In online monitoring systems for high-voltage bushing insulation indicators, the correction of the influence of power network unbalance determines the usefulness of the obtained results in assessing the condition of the bushings. Calibration is necessary to compensate for constant errors introduced by individual system components. The uncertainties of voltage transformer parameters and the influence of temperature should be taken into account in the uncertainty budget.

In the calibrated measurement system, under real conditions at the power station, it is possible to obtain the measurement uncertainty of the dielectric loss factor tgδ of no more than 0.02% in absolute conventional percentage units, which is the traditional unit for expressing this factor. In a calibrated measuring system with reference voltage measurement on voltage transformers, the uncertainty of C_1 capacitance measurements can be kept within a maximum of 2pF. However, the lack of calibration significantly increases the tgδ measurements uncertainty, resulting in values of even 10 or 15 times bigger to the value of 0.2% or 0.3%. The uncertainty of C_1 measurement increases then to +/-4pF.

REFERENCES

[1] CIGRE WG A2.43, "*Transformer Bushing Reliability*", TR 755, February

[2] Kane C.F., Golubiev A.A., Selber A.B., "*On line monitoring systems for bushings*", ISBN 0-7803-9145-4, IEEE 2005

[3] Stirs T., Skrzypek R., Tenbohlen S., "*On line condition monitoring and diagnosis for power transformers their bushings, tap changer, and insulation system*", CMD 2006, Changwong, Korea

[4] W.Gil, P. Wronek „New ideas and trends in on-line power transformer monitoring", CIGRE A2 Group colloquium, Cracow 1-6 oct. 2017

[5] Abeywickrama N., Benigtsson T., Penayo F., ."*Influence of temperature variation on transformer bushing monitoring*", art. D1-104, 48 CIGRE e-Session, Paris 2020

Wiesław Gil, Wiktor Masłowski, Measurement Uncertainty in On-line Bushing Monitoring, Journal of Energy, vol. 73 Number 1 (2024), 14–17
https://doi.org/10.37798/2024731509

Journal of Energy
VOLUME 73 Number 1 | 2024
journal homepage: http://journalofenergy.com/

Improving the Reliability of Online Bushing Monitoring

Vedran Jerbić, Samir Keitoue, Jurica Puškarić, Ivan Tomić

***Summary* — This paper discusses the common issue of bushing failures in power transformers and presents methods for preventing such failures through online monitoring. The paper presents a method based on the comparison of bushing leakage currents from different transformers connected to the same busbars to overcome problems with unreliable measurement results due to grid voltage imbalance or frequent transformer outages.**

***Keywords* — bushing, online monitoring, insulation diagnostic, capacitance, tan delta.**

I. Introduction

Together with windings and tap changers, bushing-related failures are among the top three major contributors to transformer failures. CIGRE study [1] analyzed 964 major transformer failures and results have shown that bushing failures cause 14.4% of all transformer failures on average. However, the share of bushing-related failures increases significantly with increasing voltage class totaling 27.8% for transformers with the highest system voltage from 500 kV to 700 kV. It is also worth mentioning that failures originating in the bushings most often lead to severe consequences such as fires and explosions (Fig 1).

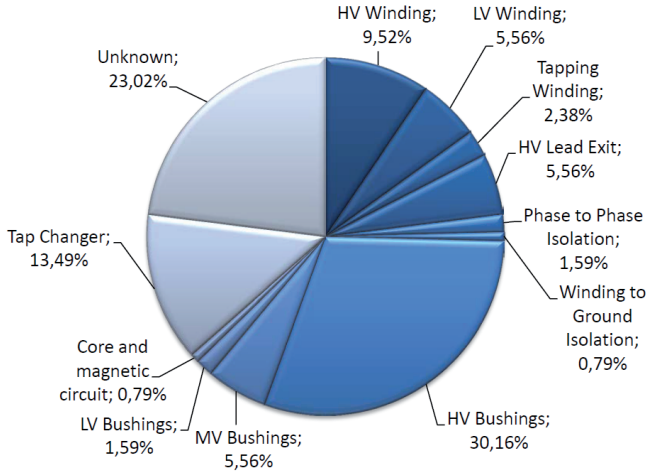

Fig. 1. Failure location where fire or explosion occurred [1].

Deeper analyses on bushing reliability, where bushing failures were analyzed separately from transformer failures and included incipient and non-transformer damaging failures were conducted in another CIGRE study [2]. In case an incipient fault is discovered early enough it allows the user to schedule a transformer outage and replace, or repair, faulty bushing to prevent transformer failure. To discover the incipient fault, several bushing diagnostic techniques have been developed over the past decades and they differ based on the required transformer state (offline or online) and the frequency in which they are performed (periodic or continuous).

Commonly accepted diagnostic methods for assessment of bushing insulation state are capacitance and dissipation factor or power factor measurements. Many utilities perform these procedures on a periodic basis. Since offline measurements are performed with stable environment conditions and controlled and known voltage source, they are very precise and reliable. However, those measurements require trained personnel and equipment and must be performed while the transformer is offline. Over the last three to four decades utilities around the globe started using bushing online monitoring to assess bushing parameters while transformer is online. Online monitoring is performed while operating conditions such as voltage, load and ambient temperature dynamically change, and that has a significant impact on the precision and reliability of those measurements. There are multiple methods developed to minimize that influence and one of them is presented in this paper.

II. Online Bushing Monitoring Methods

Bushings are being monitored by connecting an additional capacitive divider on the bushing test (measuring) tap. The connection to the bushing test tap is established by using specially designed adaptors to fit different designs of test taps of various bushing types and manufacturers. In this way, it is possible to measure the leakage currents that flow through bushing insulation and calculate changes in the bushing's capacitance and power factor. The measuring path of the system is given in Fig 2.

(Corresponding author: Vedran Jerbić)
Vedran Jerbić is with the Končar - Electrical Engineering Institute Ltd., Zagreb, Croatia (e-mail: vjerbic@koncar-institut.hr)
Samir Keitoue is with the Končar - Power Transformers Ltd., Zagreb, Croatia (e-mail: skeitoue@siemens-energy.com)
Jurica Puškarić and Ivan Tomić are with the HEP Proizvodnja Ltd., HPP Gojak, Ogulin, Croatia (e-mails: jurica.puskaric@hep.hr, ivan.tomic@hep.hr)

Vedran Jerbić, Samir Keitoue, Jurica Puškarić, Ivan Tomić, Improving the Reliability of Online Bushing Monitoring, Journal of Energy, vol. 73 Number 1 (2024), 18–23
https://doi.org/10.37798/2024731511

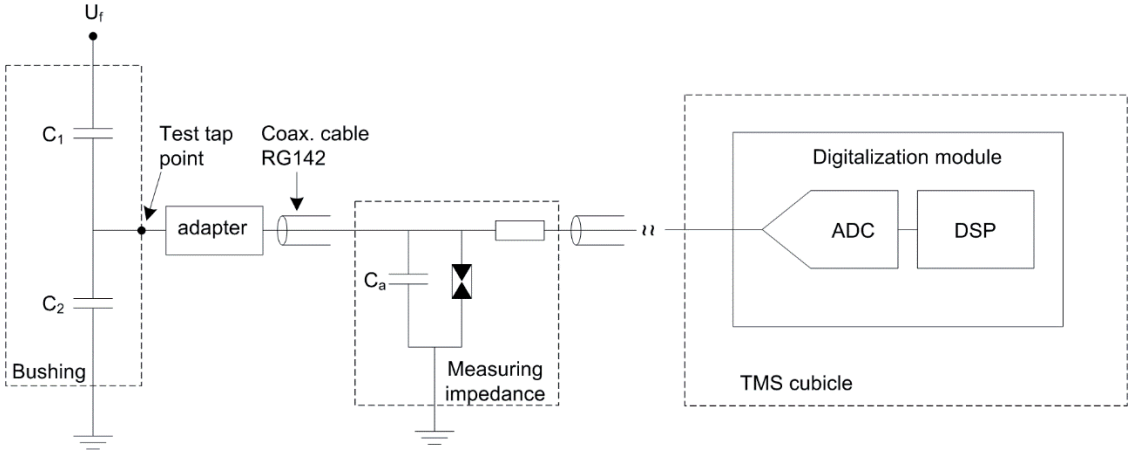

Fig. 2. Bushing and transient overvoltage monitoring measurement path

Currently there are three major methods and topologies used for bushing monitoring and each has its pros and cons speaking in terms of results reliability, complexity, and installation expenses. They are shown in Fig 3. Please note that the naming of methods may differ between different bushing monitoring vendors.

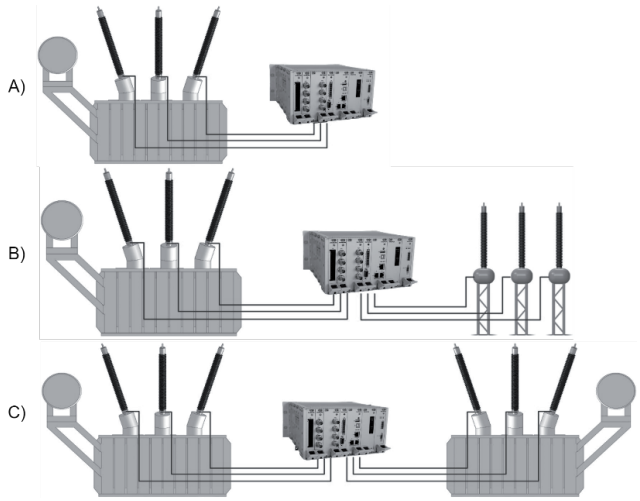

Fig. 3. Bushing monitoring methods
A) Three Phase bank; B) VT reference method; C) Dual transformer method

The simplest and most common method is three phase bank method which uses signals from three bushings connected to the same three phase bank. The most popular algorithms are the sum of currents, adjacent phase to phase, etc. These algorithms are based on comparing initial state or fingerprint data of leakage currents phase angle and amplitude with recent measurements. Using some mathematics, it is possible to calculate capacitance and dissipation factor changes. Capacitance change is expressed as a relative change from the initial state ΔC/C and dissipation factor as an absolute change Δtgδ from the initial state. The algorithms are based on the following assumptions:

- Only one out of three bushings is faulty at the time.
- The voltage level fluctuates on all three bushings similarly at the same rate.
- Angles between phase voltages do not change significantly from the initial state.

The first condition is typically fulfilled. Due to the constant changes in grid voltage levels, load, and phase angles, the latter two conditions are sometimes not fulfilled or are partially fulfilled. The accuracy and reliability of the algorithm depends on how well those conditions are met. Measured values can be expressed as a superposition of real changes in bushing parameters and error caused by grid imbalance.

$$\frac{\Delta C_{measured}}{C_0} = \frac{\Delta C_{real}}{C_0} + CAP\_ERR_{GRID} \quad (1)$$

$$\Delta tg\delta_{measured} = \Delta tg\delta_{real} + TG\_ERROR_{GRID} \quad (2)$$

In case of an unbalanced load or a fault in the grid, false alarms can appear because the angle and amplitude of grid voltage phases can change. To minimize those issues, algorithms use long averaging and other statistical analysis. Long averaging affects the response of the system which can be days or weeks. But even with that, there are cases where those algorithms do not provide satisfactory results and other methods must be used.

The other two methods previously mentioned in Fig 3 are reference based. These are VT (voltage transformer) or dual transformer methods. Measurements from a reference object, VT, or another transformer connected on the same busbar, are used to compensate for grid imbalance. Reference methods significantly improve dynamic response, accuracy, and reliability of measurement since previously mentioned conditions are no longer required.

As can be seen in Fig 3 B) and C), all signals from the device under test and reference object are connected to the same acquisition unit. This simplifies the synchronization of measurements from reference object and device under test but at the same time complicates cabling and introduces problems such as ground isolation. Very often there are no free secondary terminals of VT or other transformer in a substation, or they are far away from the device under test. Because of these, in many cases, utilities decide to implement the simplest method (three-phase bank) despite its drawbacks.

III. Novel Monitoring Method

A variant of the reference method was developed that can be used for upgrading existing systems using three phase method without additional expenses and added complexity. The system uses already existing digital infrastructure such as LAN to synchronize distributed acquisition units and share measurement data used for compensating grid imbalance problems. Reference acquisition unit can be another bushing monitoring system or other third-party devices such as a power quality analyzer or SCADA. It is only important that it measures voltages and phase angles on the same busbar and that can provide data digitally.

Vedran Jerbić, Samir Keitoue, Jurica Puškarić, Ivan Tomić, Improving the Reliability of Online Bushing Monitoring, Journal of Energy, vol. 73 Number 1 (2024), 18–23
https://doi.org/10.37798/2024731511

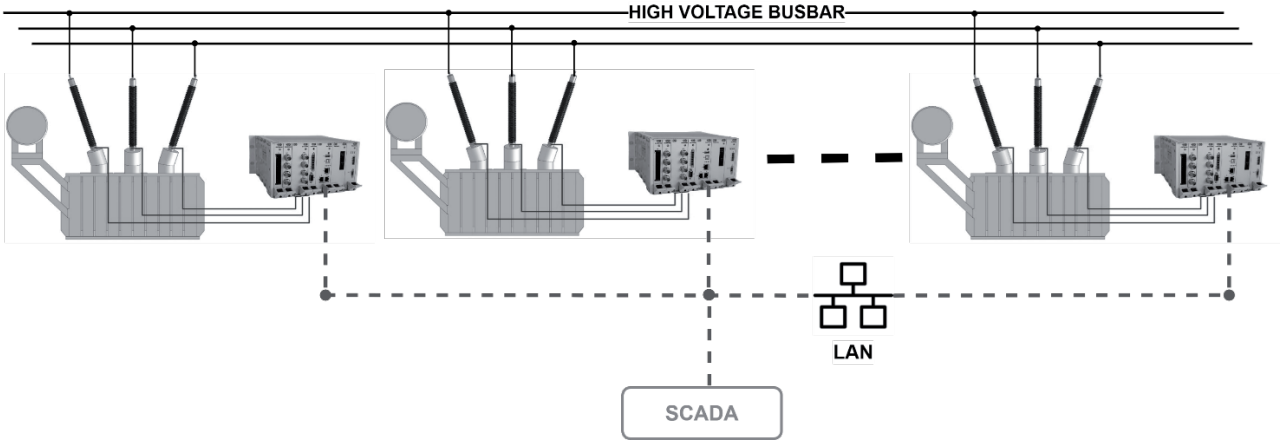

Fig. 4. New variant of the bushing monitoring reference method

Usual communication in monitoring systems is only one way. The monitoring system sends data to SCADA and does not receive any data from SCADA or other monitoring systems connected to SCADA. Existing infrastructure was used to establish bidirectional communication between all interconnected devices. Each monitoring system sends its measurements to other systems in LAN and receives data from them and SCADA.

Each unit has an operating three phase bank method used for bushing monitoring and calculates capacitance and dissipation change. Systems share calculated values, voltages, phase angles and top oil temperature readings with other systems in the same LAN. Grid imbalance compensation is performed as simple subtraction between monitored bushing and its reference bushing on another object operating on the same busbar. As the error produced by grid imbalance is the same on both the device under test and the reference object, it is canceled in subtraction. The example below explains that calculation in detail for dissipation factor measurements.

$$\Delta tg\delta_{measured,DUT} = \Delta tg\delta_{real,DUT} + TG\_ERROR_{GRID} \quad (3)$$

$$\Delta tg\delta_{measured,REF} = TG\_ERROR_{GRID}\,, \qquad \text{where } \Delta tg\delta_{real,REF} = 0 \quad (4)$$

Since it is very unlikely that bushings on both reference and device under tests, have elevated dissipation factor for same value and at the same time, one of measured values consists only of error generated by grid imbalance and other consist of error generated by grid and real change of bushing dissipation factor. This is shown by equations 3 and 4.

$$\Delta tg\delta_{real} = \Delta tg\delta_{measured,DUT} - \Delta tg\delta_{measured,REF} \quad (5)$$

Subtraction of those two equations gives final equation 5 where error produced by grid is canceled. The same principle is applied for capacitance measurements and gives the following equation.

$$\frac{\Delta C_{real}}{C_0} = \frac{\Delta C_{measured,DUT}}{C_0} - \frac{\Delta C_{measured,REF}}{C_0} \quad (6)$$

However, the key factor for subtraction is that measurements are synchronized and that bushing temperatures are more or less equal or different but stable. Different temperatures between objects can be compensated using thermal compensation curves retrieved from bushing manufacturers [3] but keep in mind that those curves are valid only for static temperature, where all insulation in bushing is at the same temperature. Bushings typically have big thermal capacitance, and in laboratory conditions will equalize to their ambient temperature after 3 – 5 hours. This is a reason why using those curves while bushing temperature is dynamically changing introduces some error.

IV. Case Study

A hydropower plant in Croatia, commonly used during peak loading, has three generators and step-up transformers. The low voltage side of each transformer is connected to its generator, and the high voltage side of transformers is connected to 110 kV busbar. A single line diagram is given in Fig. 5.

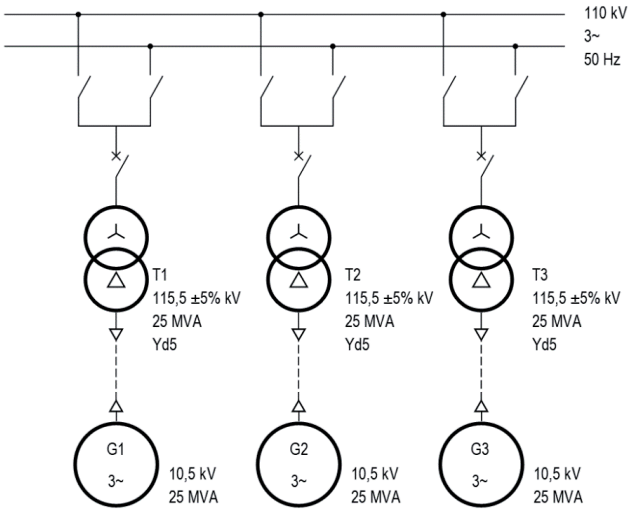

Fig. 5. Simplified single line diagram of powerplant

All three transformers were manufactured by the same company and equipped with OIP bushings of the same type and manufacturer. Transformer T1 was manufactured and commissioned in the year 2000 and transformers T2 and T3 in year 2004. Transformers T2 and T3 still have originally installed OIP bushings, while the bushing in phase U on T1 was replaced in the year 2017 (due to elevated dissipation factor) with a bushing manufactured in the year 2004 supplied as a spare one.

Table I

Production Years of Bushings

Phase	Transformer T1	Transformer T2	Transformer T3
U	2004	2004	2004
V	1999	2004	2004
W	1999	2004	2004

Considering the age of the installed bushings, the utility decided to install a bushing and transient overvoltages monitoring system in 2020. Since transformers are usually switched on only for several hours a day, and rarely more than one-week, bushing

Vedran Jerbić, Samir Keitoue, Jurica Puškarić, Ivan Tomić, Improving the Reliability of Online Bushing Monitoring, Journal of Energy, vol. 73 Number 1 (2024), 18–23
https://doi.org/10.37798/2024731511

Fig. 6. Transformer Monitoring Installation

monitoring three phase bank method was not an appropriate choice due to the slow response time.

The installed monitoring system (Končar TMS) was upgraded with the previously mentioned algorithm without the need for any hardware upgrade. The algorithm enabled canceling grid imbalance impact and provided a much faster response than commonly used algorithms with long averaging buffers and slower responses.

V. Monitoring Results

Since the monitoring system was installed on three transformers, a total of three pairs (as presented in TABLE II) of devices under test and reference objects were able to be monitored. In that way, each bushing monitoring has two reference objects for canceling grid imbalance.

Table II

Dual transformer compensation pairs

Pair	Device under test	Reference object
T1 vs. T3	T1	T3
T2 vs. T3	T2	T3
T1 vs. T2	T1	T2

Theoretically, it is possible to create 6 pairs, for example, T1 vs T3 pair can also be presented as T3 vs T1 where the device under test and reference object source swap places. In that case, the result is the same but with the opposite sign. Considering that dissipation factor and capacitance can only increase over time, negative result points that monitored parameters of the reference object have changed while positive result points that parameters of the device under test have changed. Having two references for each object is not mandatory but in this case it is important because it can be used to prove that the algorithm is effectively canceling grid imbalance and is not generating false positive alarms. For example, the pair of reference and device under test objects, whose bushings are in good condition, should have constant values of capacitance and dissipation factor over time.

Fig. 7 shows dissipation factor measurements for bushing on phase V for all pairs of DUT and reference objects. Over the displayed period, the top oil temperature was changing in the same manner on all three units. However, the bushing dissipation factor showed elevated levels and dependency versus temperature for T1 vs. T3 and T1 vs. T2 pair. The maximum measured dissipation factor change was 0.4%. That indicated that something was going wrong with the bushing on phase V on transformer T1. Values for pair T2 vs. T3, marked red on the chart above, did not change at all, which points that bushings on T2 and T3 are in good condition and proves that the algorithm effectively cancels grid imbalance impact and is not generating false alarms as previously explained.

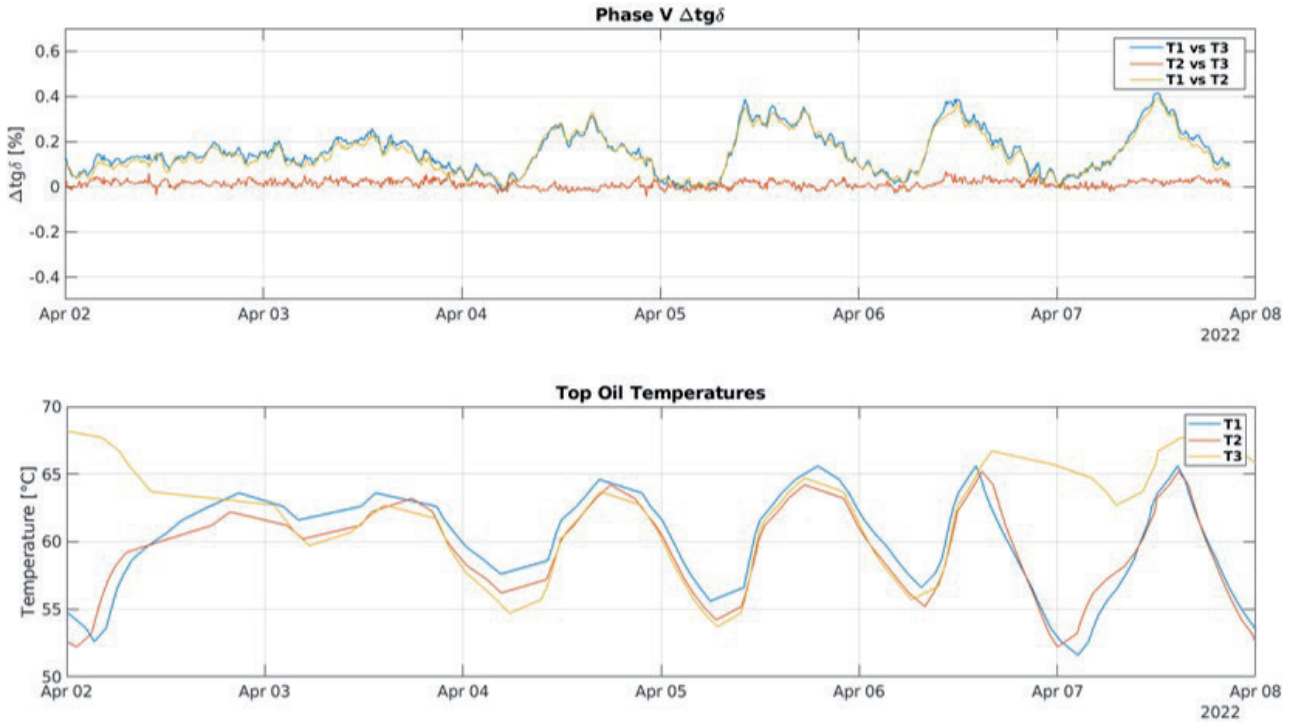

Fig. 7. Dissipation factor and temperature trend chart

Vedran Jerbić, Samir Keitoue, Jurica Puškarić, Ivan Tomić, Improving the Reliability of Online Bushing Monitoring, Journal of Energy, vol. 73 Number 1 (2024), 18–23
https://doi.org/10.37798/20247315111

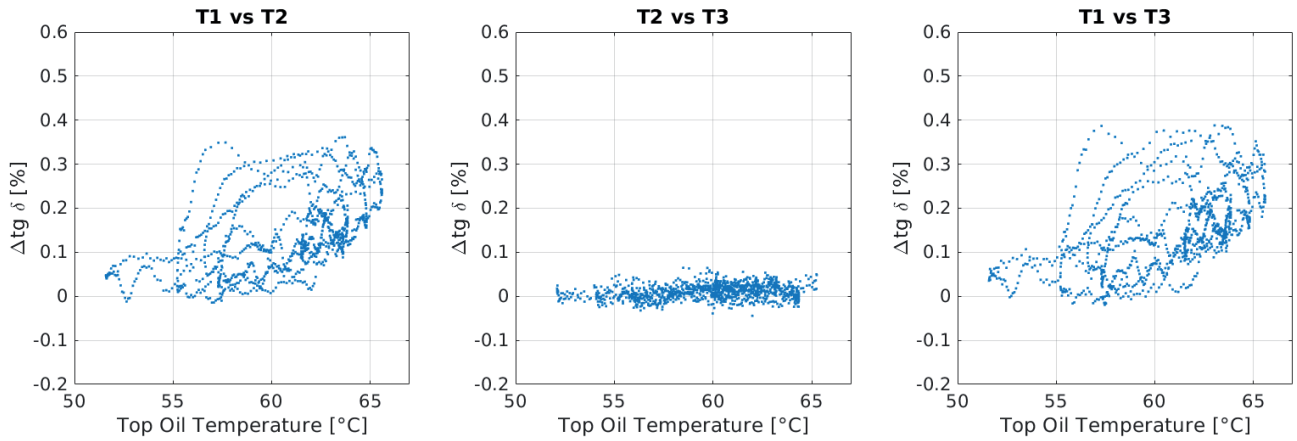

Fig. 8. Dissipation factor change versus temperature

Dissipation factor change is plotted against the top oil temperature for all three pairs and is shown in Fig. 8. It is now clear that bushing has altered dissipation factor thermal dependency which can point to moisture ingress. Dissipation factor temperature dependency is usually proven using offline measurements on low frequencies or by thermal cycling in laboratory conditions. In the summer of 2022, all bushings were checked using an offline method which proved the results obtained by the monitoring system. The bushing on phase V of the T1 transformer had a dissipation factor of 0.85% and it was immediately replaced with a new spare bushing. The utility provided faulty bushing for further postmortem analysis to prove our assumptions.

Additionally, over two years of operation, the system recorded multiple transient overvoltage and disturbance events including lightning strikes in overhead lines. This adds value to monitoring systems by enabling maintenance personnel insight into real operating conditions of bushings and transformer itself and provides valuable data for grid modelling.

Fig. 9 shows waveforms recorded during a lightning strike in the overhead line which caused 3 pole short circuit. After approximately 60 ms, automatic recloser reenergized the line. The event correlates with SCADA and LLS (lightning location system) records.

VI. Postmortem Analysis

The faulty bushing was taken to a laboratory for postmortem analysis. It was suspected that moisture in the insulation caused a dissipation factor increase and altered temperature dependency. Bushing was tested using offline method and thermally cycled in the climatic chamber from 20 to 80 °C in steps of 10°C. The bushing temperature was measured using a thermocouple on the bushing flange. After each step or increase in ambient temperature, the bushing was left for four to five hours till its temperature reached stagnation. After that bushing dissipation factor and capacitance were tested with 2 – 12 kV voltage at 50Hz frequency and by 15 – 400 Hz frequency at voltage level of 2kV.

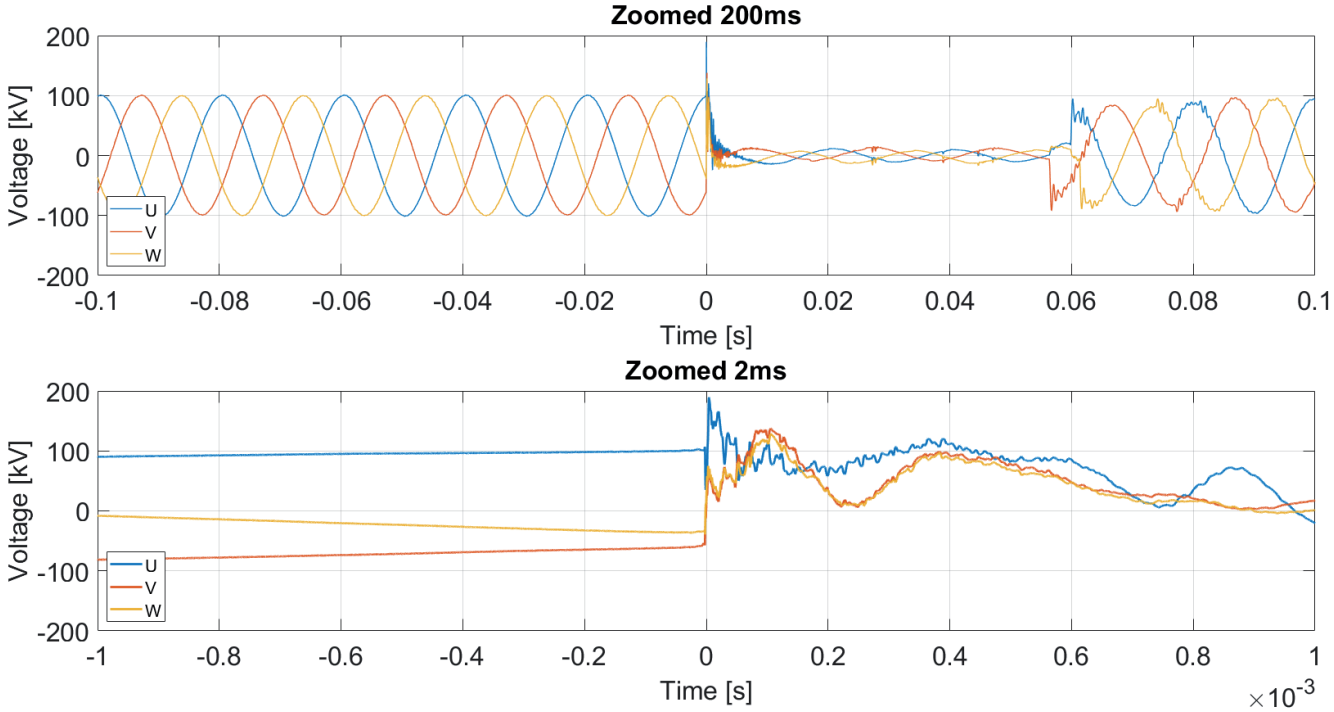

Fig. 9. Three pole short circuit caused by a lightning strike

Vedran Jerbić, Samir Keitoue, Jurica Puškarić, Ivan Tomić, Improving the Reliability of Online Bushing Monitoring, Journal of Energy, vol. 73 Number 1 (2024), 18–23
https://doi.org/10.37798/2024731511

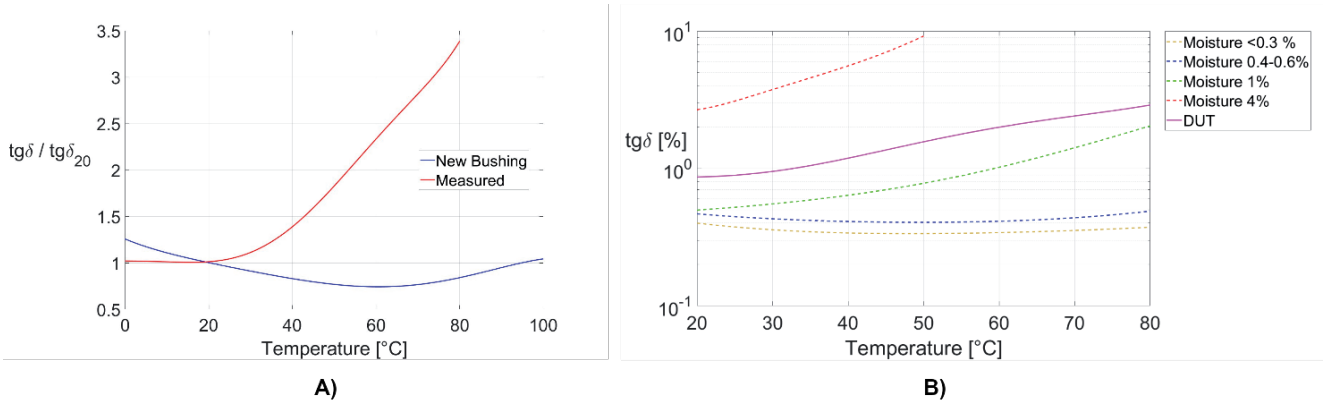

Fig. 10. Dissipation factor temperature dependency vs moisture [4]

Fig. 10 B) shows dissipation factor temperature dependency for various levels of moisture content [4] in comparison with measurements on faulty bushing (DUT). As moisture increases, the dissipation factor rises, and the saddle of the curve tends to shift to lower temperatures. Dashed curves are taken from bushing OEM datasheets and a solid pink curve was measured on faulty bushing. That proves the elevated level of moisture content. Fig. 10.A) displays the compensation factor for thermal compensation of dissipation factor measurements. The blue curve is taken from the manufacturer's datasheet and is valid only for healthy bushing. The red curve shows measurements for faulty bushing.

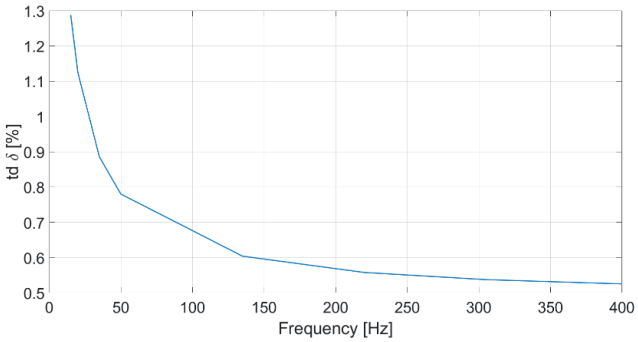

Fig. 11. Dissipation factor versus frequency

Since the dissipation factor measured at low frequencies is more dependent on moisture, those measurements are used to prove moisture ingress. Fig. 11 shows elevated values of dissipation factor at low frequencies which also points out that the bushing dissipation factor increase was caused by moisture ingress.

VII. Conclusions

The presented method provided several improvements over the simplest three phase bank method. It improved its reliability and provided up to a hundred times faster response. The faster response of the system enabled measurement of power factor temperature dependency which can be the earliest sign of moisture ingress in bushing and was not seen with other bushing monitoring algorithms. When compared with other reference methods, it has lower complexity and cost of implementation. It also provides a possibility for simple upgrades of existing monitoring systems using three phase bank method. Nevertheless, please note that even with these upgrades, the results of an online system cannot be literally compared with offline measurements since operating conditions during measurements differ significantly. Online and offline measurements should be considered as complementary methods. A reliable monitoring system should be used to trigger bushing offline measurements and enable true condition-based maintenance.

References

[1] CIGRE WG A2.37, "Transformer Reliability Survey," Technical brochure no. 642, Paris, 2016.

[2] CIGRE WG A2.43, "Transformer bushing reliability," Technical brochure no. 755, Paris, 2019

[3] A. Mikulecky, "Capacitance and dielectric dissipation factor of transformers bushings", PhD thesis (in Croatian), University of Zagreb, 2006

[4] ABB, "Bushing diagnostics and conditioning," Product information, 2750 515-142 en, Rev. 1

Vedran Jerbić, Samir Keitoue, Jurica Puškarić, Ivan Tomić, Improving the Reliability of Online Bushing Monitoring, Journal of Energy, vol. 73 Number 1 (2024), 18–23
https://doi.org/10.37798/2024731511

Journal of Energy
VOLUME 73 Number 1 | 2024
journal homepage: http://journalofenergy.com/

Is Nuclear Fusion Losing the Race with Global Warming?

Vladimir Knapp, Nikola Dragić

Summary **— According to plans for development of fusion energy, the first stage is construction of device tokamak ITER [1] with main task of establishing burning gas plasma with required stability and duration. This stage should be accomplished by 2035, starting in 2005. The next stage should be the construction of complex DEMO [2] with the task of producing all the equipment for energy production and finally producing large amounts of carbon free energy. We do not want to make predictions on the outcome of fusion program, wishing the final success to the thousands of scientists and engineers who are contributing to this heroic effort. However, there are reasons to think (Seife [18], Stork [7]) that the time is too short. Starting with a planned date of end of work with ITER by 2035, we estimate that one needs to add 25 years for development of DEMO. We cannot see production of fusion energy before 2060. However more reliable energy sources are recommended when our existence is in question. We have problems with remarks by Stork and Seife. If solar, wind and hydro energy, and nuclear fission with high safety reactors can be deployed earlier than fusion, it must have a preference.**

Keywords**— nuclear fusion, DEMO, ITER, tokamak, nuclear fission, PWR, molten salt reactors, solar energy, OTEC, global warming, climate change**

I. Introduction

Planning a concise observation, it is firstly to mention on information that ITER project with tokamak-type devices and the realization of the fusion reaction is planned to be achieved in 2035. Here, it will not be widely commented on this time projection, convinced that it is in the nature of scientific work that the outcome cannot be precisely determined. This article and our considerations are limited to tokamak systems and do not consider inertial systems due to unsolved problems of required high repetition laser.

Tokamak is the way of stabilizing plasma by combination of two magnetic fields, one along the axis of symmetry of the torus and the other field perpendicular to it, Figure 1. Tokamak is the Russian name for a type of fusion device that became dominant in the 70s when the stability of the plasma in a closed toroid was improved by several orders of magnitude. In tokamak device plasma is confined using helical magnetic field being sum of poloidal magnetic field component (toroidal plasma electrical current and poloidal external coils) and toroidal magnetic field component produced by external toroidal field coils, Figure 2. Injected neutral particles and ions and radio-frequency excitation are used for plasma heating.

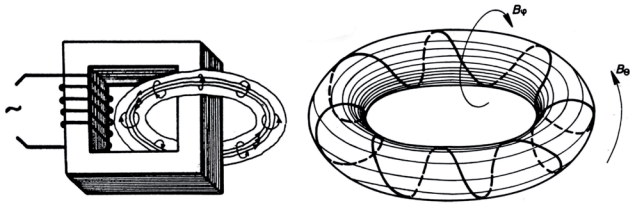

Fig. 1. Schematic diagram shows a transformer in which the secondary coil represents the burner heater. The main coil produces a toroidal field Bθ, the smaller one produces a perpendicular Bϕ to the main field.

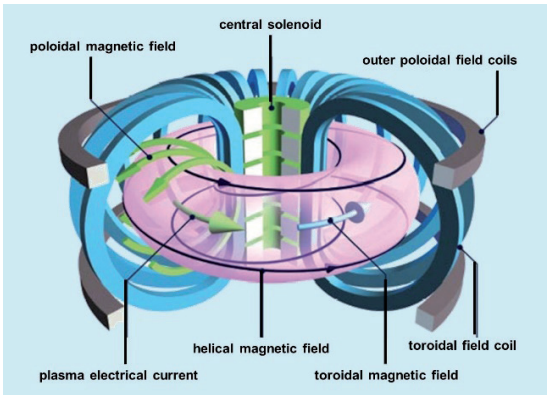

Fig. 2. ITER Tokamak magnetic field lines for plasma confinement, plasma major radius 6.2 m [28] (Figure source: https://www.iter.org/)

Based on the scientific knowledge on the ITER project, the way will be to bring the project to the end, that is, to prove that is possible to achieve stable plasma with ITER at sufficient temperature and plasma density, or, alternatively, to give a convincing denial. Therefore, it is likely that there still will be work on the fusion project with a lot of research even after the work on ITER is finished. That is why it is good that the dates in the DEMO project resulting from the Fast track strategy, the rapid development of fusion to energy production, were omitted. After the mastery and successful control of the fusion reaction in ITER, the development of the DEMO device aiming achieve energy production follows. In this phase, there is a lack of definiteness in the final phase for the same reason, requiring progress in several independent directions. It is about the introduction of many components in the chain from nuclear heat exchange to the con-

(Corresponding author: Nikola Dragić)
Vladimir Knapp is professor emeritus of the Faculty of electrical engineering and computing, Zagreb, Croatia (e-mail: vknapp@cedrus.cc.fer.hr)
Nikola Dragić is with the University of Zagreb Faculty of electrical engineering and computing, Zagreb, Croatia (e-mails: nikola.dragic@fer.hr)

Vladimir Knapp, Nikola Dragić, Is Nuclear Fusion Losing the Race with Global Warming?, Journal of Energy, vol. 73 Number 1 (2024), 24–28
https://doi.org/10.37798/2024731497

version into kinetic energy of rotation with extreme and simultaneous demands on superconductors as well as on the physics of high-temperature plasma. The problems to be faced in DEMO phase relate primarily to material properties and changes under long-term radiation with high doses of radiation.

This view of research priorities in nuclear fusion is based on years of monitoring the development of research due to the importance of fusion energy. Completion of the first phase and conditions for the realization of the fusion reaction implies a sufficient duration of stable plasma with the necessary gas plasma density. This should be achieved by 2035 according to the latest report of the general director of the ITER project [3], Bernard Bigot who recently passed away, replaced as Director general by Pietro Barabaschi.

This report is the official and authoritative document on the progress of work on the international ITER fusion development program. It is a major project that continues the development of the concept of the most successful magnetic plasma confinement in toroidal geometry to date. In this paper we do not consider alternatives to tokamak configuration before 2035.

We must give a good try to the most promising concept which was developing over several decades. After such studies promising good results, it would not be difficult to put the blame on a too early decision to start with a big project rather than with more science of plasma burning. However, the time for producing the results was short and limited. The choice was between the assumed initial successful operation of ITER as could have been achieved by 2035, and some promising but untried new geometry.

Our understanding is that alternative devices after 2035 should be oriented to use of developments applying the maximum use of DEMO technology. An entirely different approach would prolong the road to fusion and be deleted for this reason. We are about to see one of the most expensive but understandable mistakes in science, due to the pressure of date.

The authority and the science behind one of the largest international projects cannot be underestimated. But also, the question of a great new source of energy without the emission of greenhouse gases remains unanswered. Global warming threatens to seriously endanger humans within 20-30 years [4], which is shorter than the time in which we can make a decisive contribution to combating global warming if society does not mobilize without delay. When it comes to other, faster ways, we think it is interesting to look at the development of the usage of sea heat based on new estimates of the economics of OTEC [5]. OTEC could be used with double benefits of cooling the hot southern shores of the Mediterranean while producing hydrogen from sea heat. A number of solar heat conversion installations exist in tropical seas, and the economics change with rising temperatures. Mediterranean regions with warmer sea can be interesting. When it comes to endangering survival, it should be emphasized that the degree of endangerment depends on the immediate situation; large areas of Africa and Asia will be most exposed due to climate extremes and under development and poverty. Those regions require priority. But even rich countries such as the USA and Canada cannot resist a rise in global temperature above three degrees for a long time when the action and activation of feedback positive links such as the melting of the Antarctic ice, the melting of the Greenland ice, the melting of permafrost and the release of methane, large fires, conditions for the creation of hurricanes, for which the sea is warmer than 27°C.

II. Recent work on magnetic confinement fusion

The recent report on fusion work is in the publication SOFT 32nd Symposium on fusion technology was held September 18-23, 2022, in Dubrovnik, Croatia [6]. The symposium provides fresh information on the development and construction work of new equipment for tokamak. Before the last SOFT F4E conference, eight large superconducting toroidal and three poloidal coils for ITER were manufactured, among others. These are the valuable contributions of hundreds of papers from which one can have information about progress on the broad front of efforts to step by step approach the stage goal of mastering the fusion reaction. Of course, this is not the place or space for a more detailed comment on present the development of fusion, but it can be concluded that it is taking place in accordance with the plan of completion of ITER in the planned period by 2035. A long-term comprehensive program for the development of fusion energy, including the estimate of helium reserves, prepared by Derek Stork [7] allows these necessary systematic contributions to be placed in the group of necessary research.

Unfortunately, the short-term influence of nuclear magnetic fusion is unlikely, but in the long-term it is possible. The fusion device is necessarily large, like ITER, or slightly larger, due to the principled impossibility of achieving a stable plasma on small devices. In addition, we demand the simultaneous development of both low temperatures and the physics of high plasma temperatures. In addition to the well-known problem of plasma stability, we have one major problem, in inadequate resistance of materials to large doses of radiation. A problem which DEMO has to solve is the development of radiation and heat resistant materials. A critical spot for fusion with tokamak magnetic plasma confinement is radiation damage to the first wall of the chamber where the plasma burns. The key question is whether the first wall will be sufficiently resistant to ionizing radiation to withstand a huge neutron flux of energy 14.3 MeV, of the order of several times MW/m2. The fusion power plant would necessarily be large, if we do not want to lose the advantage of a smaller radial change of the magnetic field. But the dimensions of ITER are probably a balanced upper limit for a project financed from the funds of quite a number of influential participating countries [8].

Present choices for the construction of large system elements should be supported in general but the justified warning by Seife [18] should be given due attention. The design power of ITER is 500 MW, with a major plasma radius of torus of over 6 m, a large construction, and a costly investment. Considering the dimensions of ITER, the starting point of design could be the upper limit for the load on the first wall of the radiation chamber. Design value determined by many considerations, is energy flux around 10 MW/m2. If the first wall is to have a durability of 4 to 10 years, a comprehensive analytical study by 2009. Derek Stork [7] assumes a replacement time of five years and a replacement operation taking two years[1]. As can be seen, the essential characteristics of magnetic fusion device are closely related. A detailed consideration of the complex relationships of the main characteristics of the fusion power plant with tokamak magnetic limitation resulted in balanced, desirable, and physically acceptable design values of the dimensions and power of the power plant. Values are the result of numerous compromises dependent on future technological development. Long-term guidelines for this development and key dependencies are provided so that this study has lasting value.

We must consider the increasing possibility that fusion development cannot be done in time for global warming intervention, which means that we cannot use it before 2065 (2035+25+5, +required time to bring the plant to efficient operation, our estimate based on years of work with fission), based on the assumption that the DEMO device can be effective for operation in 2065. This commissioning date was obtained by adding 25 years to the information on the completion of work on ITER by 2035.

[1] It is too early to predict developments in solid states as far as 30 years in future.

Vladimir Knapp, Nikola Dragić, Is Nuclear Fusion Losing the Race with Global Warming?, Journal of Energy, vol. 73 Number 1 (2024), 24–28
https://doi.org/10.37798/2024731497

We will be able to determine the reality of this assumption only sometime after 2040. Considering the planned serial construction of fusion power plants, we must be prepared for delays. There could be various reasons for the delays. The first is in plasma combustion control. The DEMO device could be delayed, for several possible reasons, such as the unsatisfactory behavior of structural and other materials. As in fission many defects will show only in long use. Radiation would cause the change in mechanical properties, in fragility and strength and other material characteristics. For DEMO, the planned power per unit area of the active exposed electrode is about ten MW/m2, which is a huge intensity of radiation, dominantly produced by neutrons of energy 14.3 MeV. The second category of changes are changes in physical and chemical properties due to the activation of materials under massive radiation with 14.3 MeV neutrons. This again results in enormous, induced radioactivity, both in constructive materials and in most other materials. Considering a series of related project sizes, a projected surface load of 0.1 to 0.3 MW/m2 was chosen, which corresponds to the total projected maximum power flow of 500 MW from ITER.

To build a complex development as DEMO in 10 years is an impossible task. If we add 10 years, probably yes, but what do we have? It is difficult to imagine a more complex device, which is essentially dependent on the operation of all components, than the fusion power plant. The operational problems can be solved too, but that could take a much longer time. The operation of a fusion power plant would require special protective measures due to the super-intense neutron radiation. In the initial phase of operation of superconducting magnets, it would be necessary to have a number of low-temperature laboratories, equipped for quick interventions. Materials resistant to mega doses of neutron radiation, which have yet to be developed, are a much bigger problem. Assuming series of about 50 fusion power plants in operation, it would not essentially contribute to the solution of global warming, as it would be accompanied by frequent stoppages. Such a situation is expected based on the experience from the early days of fission power.

The construction of fusion power plants DEMO can be expected in the years around 2060, by being technically complete. But from the "utility use" point of view, users should see which of the utilities requirements for security and economy are acceptable or enforceable. This could cause indefinite delays. In Derek Stork's analytical study [7], the problems encountered during the construction of devices that belong to the DEMO circuit are systematically and thoroughly discussed, in as much it could be done without final dimensions of DEMO. The DEMO device is generically closely related to the development of ITER in the sense that there are many related developments when the main goal is to achieve the fusion reaction. The current perspective is that fusion will be expensive, relative to fission, at least because of the additional systems for heating the plasma and cooling the magnets. The operation of cooling devices must be reliable for long periods in an intense neutron flux. Operation at nominal fusion power should be demonstrated and verified over an extended period. An important parameter, beta [7], closely related to the strength of magnetic field, must be within the design limits according to DEMO design. Resistance to mega doses of radiation will be possible to check with a specially developed high-current neutron generator to be completed before 2035. DEMO should monitor production of tritium, the change in beta value during the operation of the power plant, and all other complex manipulations with the divertor[2]. It would serve to react to unexpected changes in the beta value. One has the impression that too many development problems were transferred to DEMO phase. Important results are expected from the Japanese tokamak JT60-SA, smaller device of tokamak type, for supporting ITER research. The development of tungsten divertors is expected. A significant contribution to development is expected from the introduction of new high-temperature superconductors.

It is to be aware of many problems and difficulties that have arisen, recently described in Charles Seife paper [18]. Even in a case that they are resolvable, they will require a lot of time for more demanding structural changes. The long-term perspective of the proposed changes is to be considered.

The general impression after reviewing the plans is that it leaves many important questions insufficiently determined, which is understandable given more than ten years since the publication of Stork's analytical text from 2009 on fusion with magnetic toroidal confinement. Considering that it will take from the concept of ITER to its final form in some thirty years, by 2035, our estimates that the work on DEMO will be completed and operational within 25 years, or up to 2060, seem optimistic. We believe that there are still too many open problems in the development of fusion on the way to an economical carbon free energy source, to be understood and accepted as a solution to global warming. We suggest that the burden of deadlines should be removed from the fusion project and that it would be free for new approaches that could have a chance to be successful in the battle against global warming. A combination with fission could be lifesaving for tokamak fusion by extending development time. We believe that the space for new ideas in energy production is decreasing, and the rich source of nuclear fission energy has been ruined by politics.

Nobel prize winner Noel-Baker conducted an early survey [9] of these unfortunate years. But for intervention by Stalin at Peace conference of 1946 the evil spirits of nuclear war would remain closed. The scientist's words of warning would not be listened to. We may recall the greatest blunder committed at the UN peace conference in 1946. Generous offer (Baruch plan) [13] by USA at UN conference in 1946, to place nuclear energy under UN control (IADA), International Atomic Development Agency. Refused by Soviet Union (already developing nuclear weapons with help of German scientist Claus Fuchs). This marked the beginning of the nuclear arms race. These are the most regrettable acts in the history of the last century. It resulted in the most dangerous nuclear arms race between the United States and the Soviet Union during the Cold War. By the 1970s the arms race was in full swing driven by military logic, almost leading to the destruction of our world.

The vast amount of physical energy, instead of being the basis of well-being for all, has become the threat of destruction for all. But despite the long-term problems with fission, especially with nuclear proliferation, nuclear fission benefices intervention is possible at least 20 years earlier than with fusion, which makes an essential difference in the fight against global warming. We must accept some long overdue decisions when using low enriched uranium. We are using low enriched uranium in many thousands of tons in peaceful use of nuclear energy. The US design of PWR reactors with containment building gives the annual probability for heavy damage to the reactor as low as 10^{-8} annually which is a high level of safety even by nuclear standards. Apart from the possibility of a person or group finding the way to doomsday cabinet, we are facing the certainty of horror and mass dying due to climate change. We should and must make the difference between uncontrollable forces of nature advancing and threatening to end the human race, and the risks that are small and controllable.

If there is a chance with the proposed intervention fission program, then any following and further development will be enabled.

[2] Electrode especially exposed to radiation, a structure from the combustion chamber, most exposed to radiation.

Vladimir Knapp, Nikola Dragić, Is Nuclear Fusion Losing the Race with Global Warming?, Journal of Energy, vol. 73 Number 1 (2024), 24–28
https://doi.org/10.37798/2024731497

III. the Construction of intervention fission power plants As a reliable and proven technology

The development of fusion power plants will experience similar problems as the development of fission power. It took many decades to develop safe fission power plants. At the same time, fission power plants are significantly simpler than fusion power plants because of the absence of complex devices for heating the plasma and cooling the magnets to low temperatures. Various defects with structural and other materials were discovered and largely resolved by monitoring the operation of fission power plants over many decades. It would be possible to build a series of about one hundred fission power plants as an international project in the next decades (2024+10+40, start of construction and operation), starting with 10 years of preparation and construction of the first power plant and ending by the completion of the construction of the last power plant during 2063-2065. At least half of these power plants could enter operation by 2050, and most by 2063-65.

With reliable technology and construction systems developed over decades, this endeavor can be accomplished and repeated using construction with established practices. There are numerous researched locations available for fast construction. The building of the fission power plant should not last longer than five years (the present situation is that many projects were experienced unjustified delays). This experience does not exist with new fusion power plants. The scientific and development capital invested in nuclear fission energy for 80 years is a unique example of development with different motives in different world regions, but which contributed to that magnificent undertaking started with the Manhattan Project in the forties of the last century in which leading American and world scientists participated. Unfortunately, politics turned that development into a nuclear arms race, but now there is an opportunity for nuclear fission energy to return with an essential contribution to the solution of the problem of global warming. Now that climate change is on the rampage, every year we gain, counts. Nuclear fission power plants could be in operation starting in 2034, which means at least some 20 years earlier than the operation of the first fusion power plant. Failure to act in a timely manner will result in an unavoidable climate catastrophe. We could gain at least 20 critical years before nuclear fusion could be ready. Who can accept responsibility for delaying feasible counter measures with proven construction of very safe fission power plants? The position of accepting the risks of fission energy instead of inevitable climate catastrophe has been discussed for many years in particularly eloquent words by James Lovelock [10] and Jim Hansen [11], leading world scientists concerned in survival.

We hope that a subjective risk assessment can change significantly now that we are already witnessing the rapid onset of disruptive climate chaos. We should understand that each year closer to 2070, we expect to see substantial changes in planned fusion energy production. Generally, we can have doubts about long energy projects starting in these years to be completed before next century. Such a planning in the next century is questionable for most long-term projects. Hope to be wrong in this pessimism but it takes some imagination to guess what is in the store for us.

Close to 440 nuclear power plants are in operation today. The last major accident involving PWR (Pressurized Water Reactor) [17] core meltdown happened in 1979[3] when a very small fraction of radioactivity escaped over border of the plant. Since then, safety of the PWR reactors has been vastly improved and the escape of radioactivity from massive containment is practically impossible. The advantage of PWR type reactors is that due to the relatively compact pressure vessel and the steam generators, they all could be placed inside very safe containment building. Radiation escape should satisfy the strictest regulations. There is only one of the possible sources of non-fossil energy, apart from abundant solar energy which needs much faster development. The next series of fission based power plants may be based on thorium reactors which are from this year in testing mode in China with a plan for more massive commercial use in following decades soon after the test phase [21]. The thorium or molten salt reactors which are promising to be more cost effective and less technical demanding with less impact on the environment providing additional safety [22].

We are entering a phase where more urgent measures are needed, but the available selection of sources is more limited.

Nuclear fission is ready and available to use while nuclear fusion is developing. Who could accept the responsibility of not supporting the construction of the first hundred safe and reliable nuclear fission PWR power plants that could be put into operation starting in 2034. That would be at least precious twenty years before the first fusion power plant could enter operation.

IV. Conclusion

Nuclear fission as a reliable and proven technology can help save the earth from climate change consequences before full-scale fusion energy is developed. We believe that this introductory text is correct in assessing the perspective of fusion. A positive outcome is possible with the ITER project and would be sufficient to support continued development of fusion. It is suggested to remove the deadlines for achieving the commercial production of fusion energy, and in the meantime to use sources without CO_2 emissions, including safe fission, under the control of the IAEA. The need to intensify the development of solar energy in all its forms exists, including ocean heat, independent from day-night cycle. As an example of what could be achieved by determined effort in years, we propose to put one hundred nuclear fission power plants into operation in the period 2034-2063/65. Highly developed intervention fission power plants of PWR type with pressure containments could enter operation at least twenty years earlier than fusion, which would be precious years in the battle against global warming. If fusion fails or is too late to use, no one can object to continued use of fission energy to counter the cause of global warming [19] [20]. Recent articles on global temperatures rise telling 2023 is the hottest year on record, with global temperatures close to the 1.5°C limit, Copernicus [25], do not give the optimism as well as the recent text on future of the fusion, P. Sutter [26]. If closing to date of decision when it must be clear that a chance of fusion source is seriously delayed beyond the chance to continue meaningful efforts to stop global warming, we have to acknowledge that clearly. The length of preparation period should be at least several years, but it cannot be shorter than five years (before 2055).

[3] Most serious accident on PWR plant occurred on the reactor from the Three Mile Island in 1979. Pressure vessel internals suffered heavy damage from partly molten reactor core, but only very small part of radioactivity escaped beyond the border of power station. In years later many improvements on containment building have additionally increased safety.

Vladimir Knapp, Nikola Dragić, Is Nuclear Fusion Losing the Race with Global Warming?, Journal of Energy, vol. 73 Number 1 (2024), 24–28
https://doi.org/10.37798/2024731497

References

[1] ITER - International Thermonuclear Experimental Reactor, https://www.iter.org/

[2] DEMO - Demonstration Power Plant, https://www.iter.org/mag/3/22

[3] Statement on the ITER progress, report by (late) Bernard Bigot, Director general, 2020. ITER Organization. Special issue 7, Available at: https://www.iter.org/multilingual/io/7/337

[4] IPCC Report, Climate Change 2022: Mitigation of Climate

Change, https://www.ipcc.ch/report/ar6/wg3/

[5] Recent progress in the economics of ocean thermal energy conversion (OTEC): Critical review and research agenda, Jannis Langer, Jaco Quist, Kornelis Blok, https://www.sciencedirect.com/science/article/pii/S1364032120302513

[6] 32nd Symposium on Fusion Technology, 18th – 23rd September 2022 in Dubrovnik, Croatia, https://soft2022.eu/

[7] DEMO and the Route to Fusion Power, Derek Stork, Euratom-UKAEA Fusion Association, Culham Science Centre, September 2009, https://fire.pppl.gov/eu_demo_Stork_FZK%20.pdf

[8] International project to develop nuclear fusion. Membership: China, European Union, Switzerland, United Kingdom, India, Japan, South Korea, Russia, United States. Partners: Australia, Canada, Kazakhstan, Thailand "WHAT IS ITER?" https://www.iter.org/proj/inafewlines

[9] Noel-Baker P. 1958. The Arms Race-A programme for World disarmament, John Calder Ltd, London

[10] James Lovelock, The Selfish Greens, Talk at the Adam Smith Institute March 15th, 2004.

[11] Jim Hansen, (July 13, 2006), The Threat to the Planet, The New York Review of Books, 53 [10].

[12] Knapp V. and Pevec D. 2018, Promises and limitations of nuclear fission energy in combating climate change. Energy Policy 120, 94-99. https://www.sciencedirect.com/science/article/abs/pii/S0301421518303318

[13] B. Baruch plan, June 14, 1946, https://www.atomicarchive.com/resources/documents/deterrence/baruch-plan.html

[14] Biello D., 2016. Carbon Capture May Be Too Expensive to Combat Climate Change. Scientific American 314, 59-65. https://www.scientificamerican.com/article/carbon-capture- may-be-too-expensive-to-combat-climate-change/

[15] "CO2 emissions", Our World in Data , by Hannah Ritchie and Max Roser, 2023, https://ourworldindata.org/co2-emissions

[16] 2021 United Nations Climate Change Conference, under Outcomes

https://en.wikipedia.org/wiki/2021_United_Nations_Climate

_Change_Conference[17] Pressurized water reactor, https://en.wikipedia.org/wiki/Pressurized_water_reactor

[18] World's Largest Fusion Project Is in Big Trouble, New Documents Reveal, Scientific American, Charles Seife, June 2023, https://www.scientificamerican.com/article/worlds-largest-fusion-project-is-in-big-trouble-new-documents-reveal/

[19] McKinsey's Global Energy Perspective, What will it take for nuclear power to meet the climate challenge? March 21, 2023 https://www.mckinsey.com/industries/electric-power-and-natural-gas/our-insights/what-will-it-take-for-nuclear-power-to-meet-the-climate-challenge

[20] COP28 – Nuclear for Climate Position Paper 2023, 25 July 2023, ENS N4C https://www.euronuclear.org/nuclear-for-climate/cop28-nuclear-for-climate-position-paper-2023/

[21] Operating permit issued for Chinese molten salt reactor, 15 June 2023, World Nuclear News, https://www.world-nuclear-news.org/Articles/Operating-permit-issued-for-Chinese-molten-salt-reactors

[22] Thorium's Long-Term Potential in Nuclear Energy, www.iaea.org/bulletin/thoriums-long-term-potential-in- nuclear-energy, IAEA bulletin 09/2023

[23] Global energy perspectives to 2060 – WEC's World Energy Scenarios 2019, T. Kober, H.-W. Schiffer, M. Densing, E. Panos, https://www.sciencedirect.com/science/article/pii/S2211467X20300766

[24] World Energy Outlook 2023, IEA International Energy Agency, https://www.iea.org/reports/world-energy-outlook-2023

[25] Copernicus, January 9, 2024, Global climate highlights, https://climate.copernicus.eu/copernicus-2023-hottest-year-record

[26] We've been 'close' to achieving fusion power for 50 years. When will it actually happen?, January 14, 2024, Paul Sutter, Stony Brook, Flatiron Institute https://www.space.com/when-will-we-achieve-fusion-power

[27] Pugwash, Pugwash Conferences, https://pugwash.org/

[28] The first fusion reactor: ITER, D.J. Campbell http://dx.doi.org/10.1051/epn/2016504

Vladimir Knapp, Nikola Dragić, Is Nuclear Fusion Losing the Race with Global Warming?, Journal of Energy, vol. 73 Number 1 (2024), 24–28
https://doi.org/10.37798/2024731497

ENERGIJA